

Article

Ultramicrosized *N*-Palmitoylethanolamine Regulates Mast Cell-Astrocyte Crosstalk: A New Potential Mechanism Underlying the Inhibition of Morphine Tolerance

Alessandra Toti ¹, Laura Micheli ¹, Elena Lucarini ^{1,*}, Valentina Ferrara ¹, Clara Ciampi ¹, Francesco Margiotta ¹, Paola Failli ¹, Chiara Gomiero ², Marco Pallecchi ³, Gianluca Bartolucci ³, Carla Ghelardini ¹ and Lorenzo Di Cesare Mannelli ¹

¹ Department of Neuroscience, Psychology, Drug Research and Child Health—NEUROFARBA—Pharmacology and Toxicology Section, University of Florence, Viale Pieraccini 6, 50139 Florence, Italy

² Epitech Group SpA, Via Luigi Einaudi 13, 35030 Padua, Italy

³ Department of Chemistry, University of Florence, Via Ugo Schiff 6, 50019 Florence, Italy

* Correspondence: elena.lucarini@unifi.it; Tel.: +39-055-2758395

Abstract: Persistent pain can be managed with opioids, but their use is limited by the onset of tolerance. Ultramicrosized *N*-palmitoylethanolamine (PEA) in vivo delays morphine tolerance with mechanisms that are still unclear. Since glial cells are involved in opioid tolerance and mast cells (MCs) are pivotal targets of PEA, we hypothesized that a potential mechanism by which PEA delays opioid tolerance might depend on the control of the crosstalk between these cells. Morphine treatment (30 μ M, 30 min) significantly increased MC degranulation of RBL-2H3 cells, which was prevented by pre-treatment with PEA (100 μ M, 18 h), as evaluated by β -hexosaminidase assay and histamine quantification. The impact of RBL-2H3 secretome on glial cells was studied. Six-hour incubation of astrocytes with control RBL-2H3-conditioned medium, and even more so co-incubation with morphine, enhanced CCL2, IL-1 β , IL-6, Serpina3n, EAAT2 and GFAP mRNA levels. The response was significantly prevented by the secretome from PEA pre-treated RBL-2H3, except for GFAP, which was further upregulated, suggesting a selective modulation of glial signaling. In conclusion, ultramicrosized PEA down-modulated both morphine-induced MC degranulation and the expression of inflammatory and pain-related genes from astrocytes challenged with RBL-2H3 medium, suggesting that PEA may delay morphine tolerance, regulating MC-astrocyte crosstalk.

Keywords: morphine; tolerance; *N*-palmitoylethanolamine; mast cell; glial cells; cross-talk



Citation: Toti, A.; Micheli, L.; Lucarini, E.; Ferrara, V.; Ciampi, C.; Margiotta, F.; Failli, P.; Gomiero, C.; Pallecchi, M.; Bartolucci, G.; et al. Ultramicrosized *N*-Palmitoylethanolamine Regulates Mast Cell-Astrocyte Crosstalk: A New Potential Mechanism Underlying the Inhibition of Morphine Tolerance. *Biomolecules* **2023**, *13*, 233. <https://doi.org/10.3390/biom13020233>

Academic Editor: Salvatore Cuzzocrea

Received: 2 December 2022

Revised: 10 January 2023

Accepted: 13 January 2023

Published: 25 January 2023



Copyright: © 2023 by the authors. Licensee MDPI, Basel, Switzerland. This article is an open access article distributed under the terms and conditions of the Creative Commons Attribution (CC BY) license (<https://creativecommons.org/licenses/by/4.0/>).

1. Introduction

Pain management is still one of the most significant problems that affect patient quality of life [1]. Pain can result from injury [2], surgery [3] or disease, such as type 1 and 2 diabetes, osteoarthritis as well as cancer [4–6] and it can also arise as a side effect of anti-cancer chemotherapies [7]. Therapies for pain relief depend on the intensity or persistence of pain; for mild pain acetaminophen, non-steroidal anti-inflammatory drugs (NSAIDs) such as aspirin, ibuprofen and naproxen are recommended, while in the case of severe pain, opioids such as morphine are the first choice [8].

The analgesic effect of morphine is mainly exerted by μ -receptor [9], although morphine also interacts, albeit weakly, with the κ and δ receptors [10]. Morphine receptors are distributed in the peripheral and central nervous system (PNS and CNS), especially in the periaqueductal gray matter and posterior horns of the spinal cord, but they are also present in different peripheral tissues and organs, being responsible for several side effects, including vomiting, nausea, constipation, pruritus, and respiratory depression. These effects typically arise within the first weeks of treatment and are likely to become more severe with time, when cognitive failure, tolerance and addiction may develop [11].

In particular, tolerance is defined as the necessity to increase the dose of morphine in order to obtain a good analgesic effect after repeated treatment and can be managed with opioid rotation, as long as the side effects do not lead to treatment withdrawal [12]. In recent decades, morphine tolerance has been attributed to the desensitization/internalization of μ -receptors and the involvement of glial cell overactivation has been recently suggested [13,14].

Glial cells (i.e., astrocytes and microglia together with oligodendrocytes and Schwann cells), not only exert supportive functions, but are increasingly considered to play a pivotal role in the transmission of pain and regulation of numerous pathophysiological processes [15–17]. In rats daily administered with morphine 10 mg/kg i.p. a significant increase in the number of glial cells was observed in the dorsal horn of the spinal cord, once tolerance has developed (i.e., after 6 days) [18]. Accordingly, it has been recently demonstrated that glial selective inhibitors as fluorocitrate, minocycline, propentofylline, and pentoxifylline delay morphine tolerance [19–22].

N-palmitoylethanolamine (PEA) is a glia modulator and a pro-homeostatic lipid mediator, belonging to the family of fatty acid ethanolamines, which are produced on demand from the lipid bilayer [23]. Recent studies have demonstrated the efficacy of PEA against persistent pain [24] and neurological disorders [25] with an optimal safety profile in humans [26]. Increasing information is currently available on the pleiotropic mechanism of action of PEA, which behaves as a cannabinomimetic compound, stimulating the effects of endocannabinoids through the so-called entourage effect [27]. Moreover, PEA is an agonist of the peroxisome proliferator-activated receptor type α (PPAR- α), a nuclear transcription factor able to inhibit both pro-inflammatory cytokine release [28] and the activity of enzymes such as cyclooxygenase [29]. In a model of chronic constriction injury, we have previously demonstrated that pain-relieving effects of PEA depend, at least in part, on a PPAR- α -mediated mechanism [30].

Notably, treatment with a bioavailable PEA formulation (i.e., ultramicrosized PEA) was shown to delay the onset of morphine tolerance and prevent the increase of glial cells number in the dorsal horn of the spinal cord [18]. The mechanisms sustaining this effect of PEA are still unclear. It is known that morphine activates mast cells (MCs) *in vivo* and enhances histamine release [31–33], while PEA down-modulates MC degranulation [34] and astrocyte activity [35].

Based on this background, the aim of the present study was to investigate if a crosstalk exists between astrocytes and MCs during morphine treatment and if PEA can regulate it. Despite the well-known limitations of 2D cell cultures, the present study might provide novel insights in the mechanism(s) underlying PEA-induced delay of morphine tolerance and non-neuronal cell(s) mainly involved in. The results could thus improve our understanding on the management of opioid tolerance and related neuroinflammatory disorders.

2. Materials and Methods

2.1. Materials

Ultramicrosized PEA (99.9% powder particle size <6 μ m) was kindly provided by Epitech Group (Saccolongo, Italy) and for simplicity will be referred to as PEA hereafter. PEA was dissolved in dimethyl sulfoxide (DMSO, Merck, Milan, Italy) at 10 mM, and 100 μ M was used with a final concentration of 1% DMSO. Morphine hydrochloride was purchased from S.A.L.A.R.S. (Como, Italy) and dissolved in sterile water.

2.2. Animals

The Sprague-Dawley rats were purchased from the Envigo company (Varese, Italy) around the seventeenth day of pregnancy. They were housed in a 26 cm \times 41 cm cage at the Laboratory Animal Housing Center (Ce.SAL) of the University of Florence, fed with a standard diet and water *ad libitum* and kept at 23 \pm 1 $^{\circ}$ C with a light cycle/12 h dark, with light at 7 am. The rats were kept alive until delivery and the pups were sacrificed

between day 1 and day 3 of life to isolate a primary culture of rat cortical astrocytes. All handling of animals were carried out in accordance with the guidelines of the European Community for the care of animals (DL 116/92, application of the directives of the Council of the European Community of 24 November 1986; 86/609/EEC). The ethics policy of the University of Florence complies with the decree Guide for the Care and Use of Laboratory Animals of the US National Institutes of Health (NIH Publication number 85-23, revised 1996; University of Florence assurance number: A5278-01). Formal approval to conduct the experiments described was obtained from the Italian Ministry of Health (No. 333/2020-PR) and from the Animal Subjects Review Board of the University of Florence. All efforts were made to minimize animal suffering and reduce the number of animals used.

2.3. Cell Culture

The rat basophilic leukemia cells (RBL)-2H3, purchased from American Type Culture Collection (ATCC, Manassas, VA, USA), were cultured in Eagle's Minimum Essential Medium (EMEM)-High Glucose growth medium (ATCC, Manassas, VA, USA), containing L-glutamine (2 mM), supplemented with 15% Heat Inactivated Fetal Bovine Serum (FBS, Euroclone, Milan, Italy), penicillin (100 U/mL) and streptomycin (100 µg/mL; Merck, Milan, Italy). The RBL-2H3 cell line was used as a commonly accepted model of MCs [36].

Primary cultures of cortical astrocytes were obtained according to the method described by McCarthy and de Vellis [37]. Briefly, the cerebral cortex of new-born Sprague-Dawley rats (Envigo, Varese, Italy) post-natal day 1–3 was dissociated in Hanks balanced salt solution containing 0.5% trypsin, 0.2% EDTA and 1% DNase (Merck, Milan, Italy) for 30 min at 37 °C. The suspension was mechanically homogenized and filtered with 70 µm filters. Cells were plated in Dulbecco's Modified Eagle's Medium (DMEM)-High Glucose (Merck, Milan, Italy) supplemented with 20% FBS (Euroclone, Milan, Italy), L-glutamine (2 mM), penicillin (100 U/mL) and streptomycin (100 µg/mL; Merck, Milan, Italy). Confluent primary glial cultures were used to isolate astrocytes, removing microglia and oligodendrocytes by shaking. After 21 days of culture, astrocytes were plated according to experimental requirements. Cells were maintained in incubator, at 37 °C, and in a humidified atmosphere of 5% CO₂.

2.4. Cell Viability Assay

The RBL-2H3 cells and astrocytes were plated at the density of 4×10^3 and 5×10^3 cells/well respectively in a 96-well plate. After the appropriate treatments at 24 and 48 h, the medium was removed and the cells incubated with a 1 mg/mL solution of Thiazolyl Blue Tetrazolium Bromide (MTT; Merck, Milan, Italy), at 37 °C, for 1 h and a half. The dissolution of the crystals was carried out with 200 µL of DMSO per well, and the absorbance was read at 590 nm using the EnSight Multimode Plate Reader (Perkin Elmer) [38].

2.5. Cell Count

The RBL-2H3 cells were plated in 6-well plate, at a density of 4×10^5 cells/well, sensitized with anti-DNP IgE (50 ng/mL) and concurrently treated with PEA 100 µM. After 24 and 48 h, cells were detached and counted using a Burker's chamber. A mean of two counts for condition with 4 replicates were analyzed [39].

2.6. β -hexosaminidase Assay

The RBL-2H3 cells were plated in a 24-well plate, at a density of 5×10^4 cells/well, and the next day cells were sensitized with anti-dinitrophenyl (DNP)-IgE (50 ng/mL) at 37 °C overnight. After 18 h, two washes with modified Tyrode's (MT) buffer (20 mM HEPES, 135 mM NaCl, 5 mM KCl, 1.8 mM CaCl₂, 1 mM MgCl₂, 5.6 mM glucose, and 0.05% BSA, pH 7.4) were performed and then cells were treated in 250 µL of MT buffer containing morphine 30 µM, PEA 10–100 µM or morphine 30 µM + PEA 100 µM for 30 min at 37 °C. Cells were then stimulated with DNP-BSA (625 ng/mL) for 5, 10, 15 and 30 min at 37 °C.

After stimulation, the supernatant was collected and the cells lysed with 250 μ L of MT buffer containing 0.1% Triton X-100, and then sonicated for 30 s on ice. Both supernatants and cell lysates were transferred to a new 96-well plate, 50 μ L per sample, and incubated for 1 h at 37 °C with 50 μ L/well of 1 mM p-nitrophenyl-N-acetyl-d-glucosaminide (NAG; Merck, Milan, Italy) dissolved in 0.1 M citrate buffer (pH 4.5). The enzymatic reaction was then stopped by adding 100 μ L/well of 0.1 M carbonate buffer (pH 10.0). The absorbance (A) was read at 405 nm using EnSight Multimode Plate Reader (Perkin Elmer). The percentage of β -hexosaminidase released was calculated as follows: $100 \times [(A_{\text{supern}} - A_{\text{white}})/(A_{\text{supern}} - A_{\text{white}}) + (A_{\text{pellet}} - A_{\text{white pellet}})]$ [40].

2.7. Histamine Assay

The amount of histamine in RBL-2H3 media was measured by isotopic dilution (ID) bidimensional high performance liquid chromatography (2D-HPLC) with tandem mass spectrometry (MS/MS) method. The instrument employed was a Varian (Palo Alto, CA, USA) triple quadrupole 1200 L system (able to perform MS/MS experiments) coupled with three Prostar 210 pumps (each one can manage one solvent line), a Prostar 410 autosampler and an electro-spray ionization (ESI) source. All the raw data collected were processed by Varian Workstation (version 6.8) software. The system was equipped with two 6-port valves. The following columns were used: (1) SeQuant[®] ZIC-HILIC 20 \times 2.1 mm as loading column and (2) SeQuant[®] ZIC-HILIC 50 \times 2.1 mm as analytic column, both with a particle size of 3.5 μ m. The elution was performed with the following solvents: (1) solvent A, mQ water:acetonitrile 9:1 solution added with 5 mM formic acid and 15 mM ammonium formate; (2) solvent B, mQ water:acetonitrile 1:9 solution added with 15 mM formic acid and 5 mM ammonium formate; and (3) solvent C (used for sample loading), mQ water:acetonitrile 1:9 solution added with 17.5 mM formic acid 2.5 mM ammonium formate. The loading time was carried out in isocratic elution with the solvent C for 2 min at flow of 0.5 mL min⁻¹. It was demonstrated that in 2 min the analyte is completely retained by the loading column. After 2 min the valve changed position and the gradient of A and solvents started in counter-flow from the loading to the analytic columns. The gradient started from 90% to 20% of solvent B in 7 min and held for 3 min, then it returned at 90% of solvent B in 0.1 min and restored the initial condition for 13 min, for a total run time of 25 min [41]. More details on the method are reported in Supplementary Materials (Tables S1–S5; Figure S1).

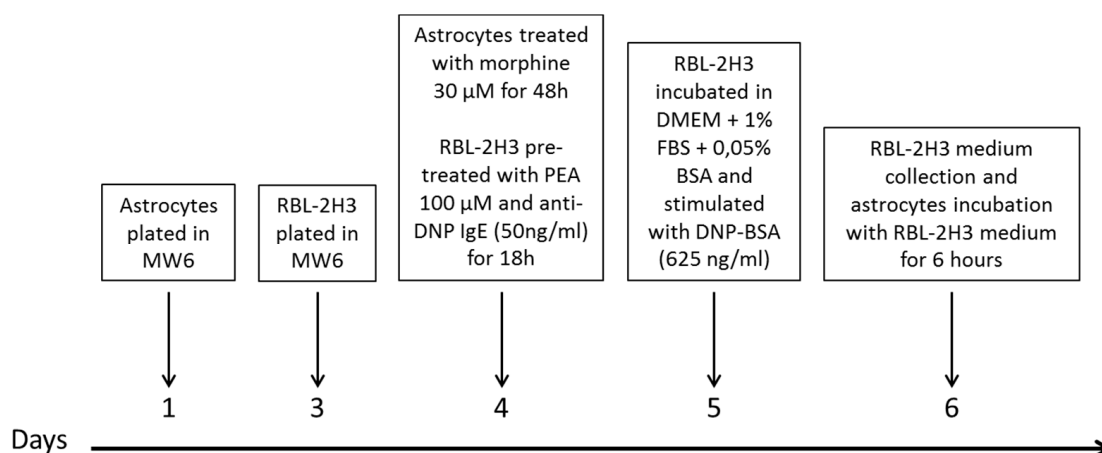
2.8. Collection of Mast Cell-Conditioned Medium

RBL-2H3 media were collected after appropriate treatment and centrifuged two times for 5 min at 200 \times g to eliminate floating cells and debris before treating astrocytes.

2.9. Timeline of Astrocytes Treatment with Mast Cell-Conditioned Medium

Primary astrocytes were plated in 6-well plate at a density of 2.5×10^4 cells/well and subsequently treated for 48 h with 30 μ M morphine in DMEM with 1% FBS. In parallel, RBL-2H3 were plated in 6-well plate at a density of 4×10^5 cells/well and pre-sensitized the next day with anti DNP-IgE 50 ng/mL \pm PEA 100 μ M.

The next day, after two washes in phosphate buffer solution (PBS) to eliminate DNP-IgE and PEA, the RBL-2H3 were incubated in DMEM with 1% heat inactivate FBS and 0.05% BSA and then stimulated for 24 h with DNP-BSA 625 ng/mL. Conditioned media of RBL-2H3 were collected as previously described. At the end of 48 h of morphine treatment, astrocytes were incubated for 6 h with media collected from control and PEA pre-treated RBL-2H3 (see Scheme 1).



Scheme 1. Experimental scheme.

2.10. Protein Extraction, Electrophoresis, and Western Blot

Cells were lysed with 50 mM Tris-HCl pH 8.0, 150 mM NaCl, 1 mM EDTA, 0.5% Triton X-100 and complete protease inhibitors (Roche, Milan, Italy).

The lysates were collected, sonicated for 3 min in ice, vortexed for 1 min and finally centrifuged at $12,000 \times g$ for 10 min, at 4 °C, and the supernatant collected. Total protein concentrations were quantified by bicinchoninic acid test (Merck, Milan, Italy). An amount of 40 µg of proteins was resolved with precast polyacrylamide gel (BOLT 4–12% Bis-Tris Plus gel; Thermo Fisher Scientific, Monza, Italy) before electrophoretic transfer to nitrocellulose membranes (Bio-Rad, Milan, Italy). The membranes were blocked with 5% Blotto, non-fat dry milk (Santa Cruz Biotechnology, Dallas, TX, USA) dissolved in PBS-0.1% Tween (PBST; Merck, Milan, Italy) and then probed overnight at 4 °C with primary antibodies specific for mouse MOR-1 (1:1000; cod. sc-515933, Santa Cruz Biotechnology, Dallas, TX, USA) and mouse GAPDH (1:5000; cod. sc-32233, Santa Cruz Biotechnology, Dallas, TX, USA). The membranes were then incubated for 1 h in PBST containing the anti-mouse secondary antibody HRP conjugated (1:5000; Santa Cruz Biotechnology, Dallas, TX, USA). ECL (Enhanced Chemiluminescence Pierce, Rockford, IL, USA) was used to visualize peroxidase-coated bands. Densitometric analysis was performed using the ImageJ analysis software (ImageJ; NIH, Bethesda, MD, USA). Normalization with housekeeping gene GAPDH content was performed [42].

2.11. Immunofluorescence

The RBL-2H3 cells and astrocytes were plated at the density of 4×10^5 and 5×10^4 cells/well respectively on 22×22 mm cover slides placed in a 6-well plate. After the appropriate treatments, the cells were fixed with 4% paraformaldehyde for 15 min at room temperature. Permeabilization was performed by incubation for 1 h with PBS 1X-0.3% Triton and blocking phase with PBS 1X-0.3% Triton+0.5% BSA followed by overnight incubation at 4 °C with rabbit anti-mast cell tryptase (1:200, GeneTex, TX, USA) or rabbit anti-glial fibrillary acidic protein (GFAP; 1:200, cod. Z0334, Dako Agilent, Santa Clara, CA, USA) diluted in the blocking solution. The next day, after appropriate washing in PBS, the slides were incubated for 2 h with the Alexa Fluor[®] 568 goat anti-rabbit conjugated secondary antibody (1:500, Life Milan, Italy) at room temperature, diluted in the blocking solution. Finally, nuclei were labeled with 4',6-diamidino-2-phenylindole (DAPI; Life Technologies, Milan, Italy) for 5 min, diluted in PBS to a final concentration of 500 ng/mL. After washing in double distilled water, the slides were placed on a specimen slide using the Fluoromount[™] aqueous mounting medium (Life Technologies, Milan, Italy). The images were acquired using a Leica DM6000 B motorized fluorescence microscope equipped with a DFC350FX camera (Leica, Mannheim, Germany). The intensity

was calculated using imageJ and analyzing 10 fields per slide acquired randomly with a 20× objective [42].

2.12. Real Time Polymerase Chain Reaction (RT-PCR)

Total RNA was isolated from cells using NucleoSpin[®] RNA (Macherey-Nagel, Düren, Germany) following manufacturer's instruction. An amount of 500 nanograms of RNA was retrotranscribed using iScript cDNA Synthesis kit (Bio-Rad, Milan, Italy). RT-PCR was performed using SsoAdvanced Universal SYBR[®] Green Supermix (Bio-Rad, Milan, Italy) following the thermal profile suggested by the kit.

The following primers were used for detection:

rSerpina3n: forward 5'-CTTTCTGCAGTATGTGGGAATCACTTGG-3' and reverse 5'-GGCTGCATTGCTCTAAGTAGGAGTGC-3' (Invitrogen);

rCCL2: forward 5'-TCTTCCTCCACCACTATGCAGGTCTC-3' and reverse 5'-TCTTTGGGACACCTGCTGCTGGTG-3' (Invitrogen);

rGFAP forward 5'-CTGACACACGTTGTGTTCAAGCAGCC-3' and reverse 5'-CTGAAGGTTAGCAGAGGTGACAAGGG-3' (Invitrogen).

Validated primers to detect rIL-6 (qRnoCID0053166), rIL-1 β (qRnoCID0004680), rEAAT2 (qRnoCED0005967), rTNF α (qRnoCED0009117), and r β 2microglobulin as house-keeping (qRnoCED0056999), were purchased from Bio-Rad (Bio-Rad, Milan, Italy). The differential expression of the transcripts was normalized on the housekeeping gene.

2.13. Measurement of Intracellular Ca²⁺

Dynamic intracellular cytosolic Ca²⁺ ([Ca²⁺]_i) was evaluated in astrocytes plated on round glass coverslips (diameter 25 mm) and after the appropriate treatments they were labeled with 4 μ M Fluo-4AM (Life technologies, Milan, Italy) for 45 min, at 37 °C. Cells were washed and kept in Hepes buffer (NaCl 140 mM, NaHCO₃ 12 mM, Hepes 10 mM, KCl 2.9 mM, NaH₂PO₄ 0.5 mM, CaCl₂ 1.5 mM, glucose 10 mM, MgCl₂ 1.2 mM, pH = 7.4). The coverslips were mounted in a perfusion chamber and placed on the stage of an inverted reflected light fluorescence microscope (Zeiss Axio Vert. A1 FL-LED) equipped with fluorescence excitation (475 nm) with LED. Cells were incubated for at least 5 min in the control solution and then stimulated with 100 μ M ATP. The dynamics of calcium was recorded for at least 3 min after administration of the agonist. The fluorescence of Fluo-4AM was recorded with a Tucsen Dhyana 400D CMOS camera (Tucsen Photonics Co., Ltd., Fuzhou, China) with a resolution of 1024 × 1020 pixels². Ca²⁺ dynamics was measured by single cell imaging analysis at 35 °C. The images were recorded using the Dhyana SamplePro software, recording 13 frames per second and dynamically analysed with the open-source community software for bioimaging Icy (Pasteur Institute, Paris, France). A signal-to-noise ratio of at least 5 arbitrary units of fluorescence (A.U) was considered as an agonist-induced increase in Ca²⁺. The following parameters were evaluated: the ratio between the agonist-induced maximum change in fluorescence and the basal fluorescence ($\Delta F/F$, measured as A.U.), the time to reach the maximum calcium value and the area under the fluorescence calibrated curve baseline (AUC/F, evaluated as A.U.). The experiments were repeated in 3 different cell preparations, analysing at least 6 cells per optical field (using a 40× magnification objective) [43].

2.14. Statistical Analysis

Results were expressed as mean \pm S.E.M. and analysis of variance (ANOVA) was performed.

A Bonferroni significant difference procedure was used as post hoc comparison. Data were analysed using the "Origin 8.1" software (OriginLab, Northampton, MA, USA). Differences among groups were considered significant at values of $p < 0.05$. * p -value < 0.05 ; ** p -value < 0.01 ; *** p -value < 0.001 .

3. Results

3.1. Morphine and PEA, Used Solely or in Combination, Do Not Affect Mast Cell Viability

We first verified by MTT test that none of the investigated concentrations of morphine (0.3–300 μM) was toxic on RBL-2H3 cells at either 24 or 48 h treatment (Figure 1a). The 30 μM concentration was therefore chosen since it was observed to induce a consistent degranulation without any toxic effects. Then, increasing concentrations of PEA (10 nM–100 μM) together with 30 μM morphine were tested on RBL-2H3 cells by MTT. Figure 1b,c show that PEA at the concentration range 10 nM–10 μM , alone or in combination with 30 μM morphine, does not affect cell viability in a significant manner, either at 24 or 48 h. Although a decrease in RBL-2H3 cell viability was observed with PEA 50 μM and 100 μM , with the effect being worsened by morphine, PEA 100 μM (24 h treatment) did not affect the cell count, suggesting that it was not toxic at the higher concentration (Figure 1d). A decrease in the number of cells was observed at 48 h, probably due to an impaired proliferation more than a toxic effect of PEA (Figure 1d). For this reason, 24 h treatment was selected for further experiments. The total protein content at 24 h in control and PEA 100 μM -treated RBL-2H3 cells confirmed the findings from the cell count assay (Figure 1e).

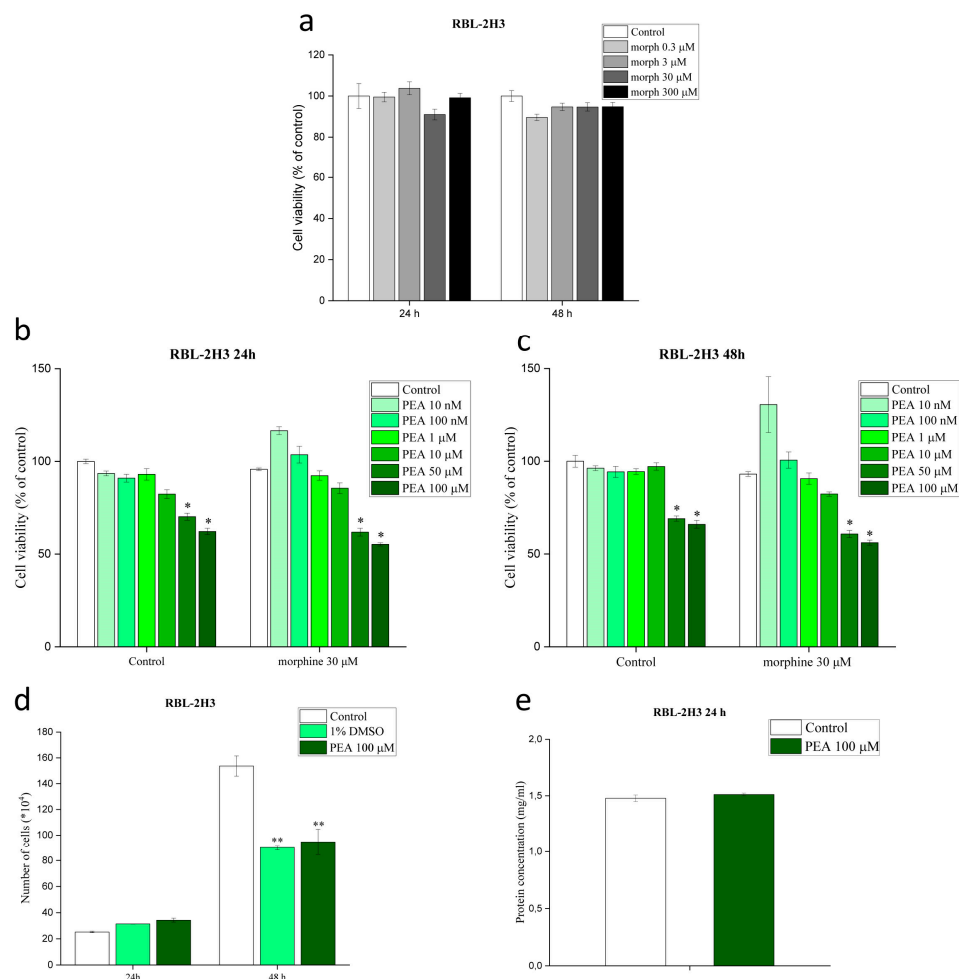


Figure 1. Effect of morphine and *N*-palmitoylethanolamine (PEA) on MC viability. (a) MTT of RBL-2H3 cells treated with increasing concentrations of morphine (0.3–300 μM) for 24 and 48 h; (b,c) MTT of RBL-2H3 treated with increasing concentrations of PEA (10 nM–100 μM) alone or in combination with 30 μM morphine for 24 and 48 h; control condition was arbitrarily set as 100%; (d) Cell count of RBL-2H3 cells treated with PEA 100 μM and 1% DMSO at 24 and 48 h; (e) Protein content in RBL-2H3 cells treated for 24 h with PEA 100 μM . Values are expressed as the mean \pm S.E.M. of three experiments. * $p < 0.05$; ** $p < 0.01$ vs. control.

3.2. RBL-2H3 Cells Express the μ -Receptor and Morphine Augments Mast Cell Degranulation

Since opioid treatment is known to activate MCs [33], but no information is available on the molecular mechanism(s), we first evaluated the expression of morphine receptors on RBL-2H3 cells. Western blot analysis of MOR-1 demonstrated, for the first time, that RBL-2H3 cells express morphine μ -receptor (Figure 2a and Figure S2). Given the consistent basal degranulation, the RBL-2H3 cell activation protocol had first to be optimized (Figure S3) before investigating morphine-induced degranulation. Similar to what reported by other groups [44,45], RBL-2H3 cells were pre-sensitized with anti-DNP IgE (50 ng/mL) for 18 h. The next day, cells were incubated with morphine (0.3–300 μ M) for 30 min in a buffer containing 0.05% BSA and then stimulated with DNP-BSA (625 ng/mL) for 10 min [46,47]. In these conditions, a controlled granule release was achieved. As reported in Figure 2b, morphine induced a concentration dependent decrease of tryptase intensity, suggesting an increased tryptase release and thus degranulation. To better investigate morphine-induced degranulation, the release of β -hexosaminidase was also studied and the percentage of β -hexosaminidase in the medium was compared to that inside the cells. A significant 15% increase in the release of β -hexosaminidase was observed in sensitized RBL-2H3 cells challenged with DNP-BSA for 5, 10, 15 and 30 min and treated with 30 μ M morphine for 30 min (Figure 2c). Lengthening morphine incubation time up to 24 h did not generate any statistically significant increase (Figure 2d), probably due to the very short time needed by morphine to induce maximum RBL-2H3 cell degranulation.

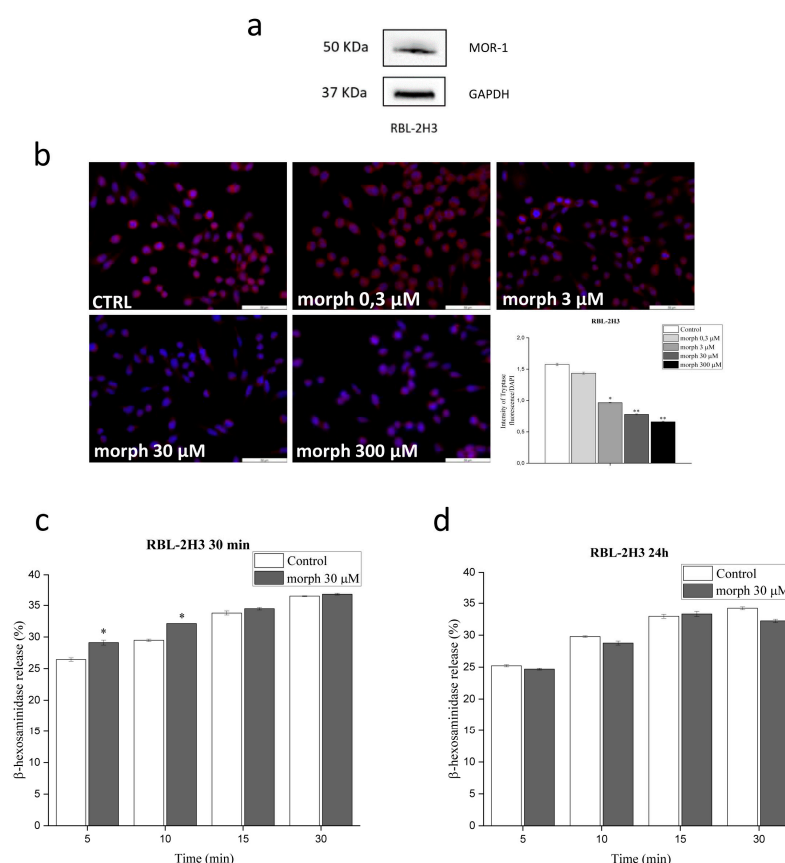


Figure 2. Effect of morphine on MC degranulation. (a) Western blot of MOR-1 (μ -receptor) on RBL-2H3 cells. The expression was compared to GAPDH levels. (b) Immunofluorescence for tryptase on RBL-2H3 cells pre-sensitized with anti-DNP IgE 50 ng/mL, treated the next day with increasing concentrations of morphine (0.3–300 μ M) for 30 min and then stimulated with DNP-BSA for 10 min. Cell nuclei were labeled with DAPI. Scale bar = 50 μ m. (c) β -hexosaminidase assay of RBL-2H3 cells pre-sensitized with anti DNP-IgE 50 ng/mL, treated for 30 min with morphine 30 μ M and stimulated with DNP-BSA for 5, 10, 15, 30 min; (d) β -hexosaminidase assay of RBL-2H3 cells pre-sensitized with

anti DNP-IgE 50 ng/mL, treated for 24 h with morphine 30 μ M and stimulated with DNP-BSA for 5, 10, 15, 30 min. DNP-BSA was used at a final concentration of 625 ng/mL in all experiments. Values are expressed as the mean \pm S.E.M. of three experiments. * $p < 0.05$; ** $p < 0.01$ vs. control.

3.3. PEA Counteracts Morphine-Augmented Mast Cell Degranulation

Since a previous *in vivo* study in rats demonstrated that one-week pretreatment with PEA enhanced the analgesic effect of morphine, thus exerting an opioid sparing effect [48], we choose to pre-treat RBL-2H3 cells with PEA during anti DNP-IgE sensitization (18 h) and then incubate cells with PEA for 30 min the following day. The incubation time and doses were based on preliminary experiments (Supplementary Material). Briefly, the β -hexosaminidase assay revealed that PEA 10 μ M was effective in reducing RBL-2H3 cell degranulation up to 40%, while PEA at 100 μ M achieved 80% reduction (Figure S4). The ability of 100 μ M PEA to counteract morphine-induced RBL-2H3 cell degranulation was analysed by β -hexosaminidase assay. RBL-2H3 cells were challenged with DNP-BSA for 5, 10, 15 and 30 min. Interestingly, the effect of PEA was found to be statistically significant not only compared to morphine, but also with regard to the DNP-BSA-challenged RBL-2H3 cells (Figure 3a). Moreover, the second pre-treatment period with PEA (100 μ M for 30 min, after the first 18 h pre-treatment) appeared not to be necessary, since the inhibitory activity was maintained after a single pre-treatment period both in the absence and presence of morphine 30 μ M (Figure 3a). To confirm these data, the level of histamine released in the medium was also quantified by HPLC with the same experimental setting. The assay allowed to identify a slight, albeit non-significant, increase in histamine concentrations in 30 μ M morphine-treated RBL-2H3 cells compared to controls. Conversely, pre-treatment with PEA 100 μ M significantly decreased histamine release, both in the absence and presence of morphine 30 μ M (Figure 3b).

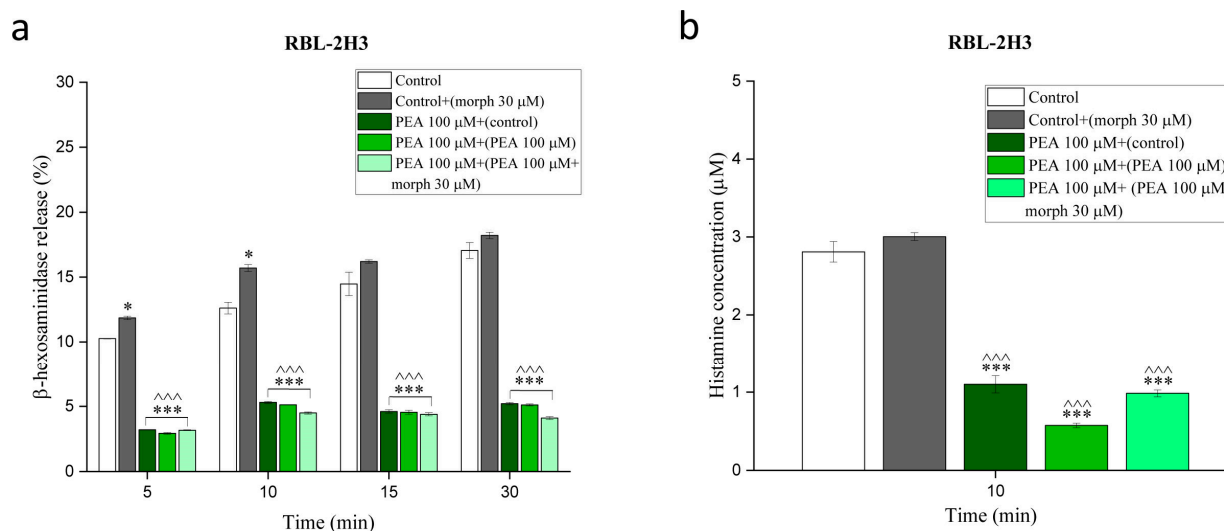


Figure 3. Effect of PEA on morphine-stimulated MC degranulation. RBL-2H3 sensitized with anti-DNP IgE 50 ng/mL and pre-treated with PEA 100 μ M for 18 h, incubated the next day with 30 μ M morphine, 100 μ M PEA, the combination of PEA and morphine and medium only, for 30 min, then stimulated with DNP-BSA for 5, 10, 15 and 30 min for β -hexosaminidase assay (a) and 10 min for histamine dosage in the medium by HPLC (b). DNP-BSA was used at a final concentration of 625 ng/mL in all experiments. Values are expressed as the mean \pm S.E.M. of three experiments. * $p < 0.05$; *** $p < 0.001$ vs. control. ^^^ $p < 0.001$ vs. control + (morphine 30 μ M).

3.4. PEA Down-Modulation of Mast Cell Degranulation Is Long-Lasting

To investigate whether down-modulation of RBL-2H3 cells by PEA (100 μ M) was long-lasting, we challenged cells with DNP-BSA for 30 min, 2, 6 and 24 h the day after

anti DNP-IgE sensitization and measured the content of histamine in the medium at every timepoint. After each challenge, PEA-treated RBL-2H3 cells released a significantly lower amount of histamine compared to controls. As shown in Figure 4a, histamine concentration (μM) in treated and control cells was respectively 2.55 ± 0.1 vs. 10.2 ± 0.13 at 30 min, 6.86 ± 0.71 vs. 15.07 ± 0.5 at 2 h, 24.57 ± 0.1 vs. 39.03 ± 0.7 at 6 h and finally 89.98 ± 0.9 vs. 126.92 ± 0.9 at 24 h. PEA 100 μM significantly increased also tryptase immunofluorescence, thus indicating a decreased degranulation (Figure 4b). Since MC activation is known to induce not only the release of pre-formed mediators (e.g., histamine) but also the release of de-novo synthesized cytokines and chemokines, the effect of PEA on newly synthesized mediators was also investigated. Using RT-PCR, we found that 18 h pre-treatment with PEA 100 μM before 6 h DNP-BSA challenge, efficiently counteracted the increase in the expression of the CCL2 (0.1 ± 0.002 vs. 1 ± 0.02) and TNF- α (0.63 ± 0.015 vs. 1 ± 0.02) genes, compared to controls (Figure 4c).

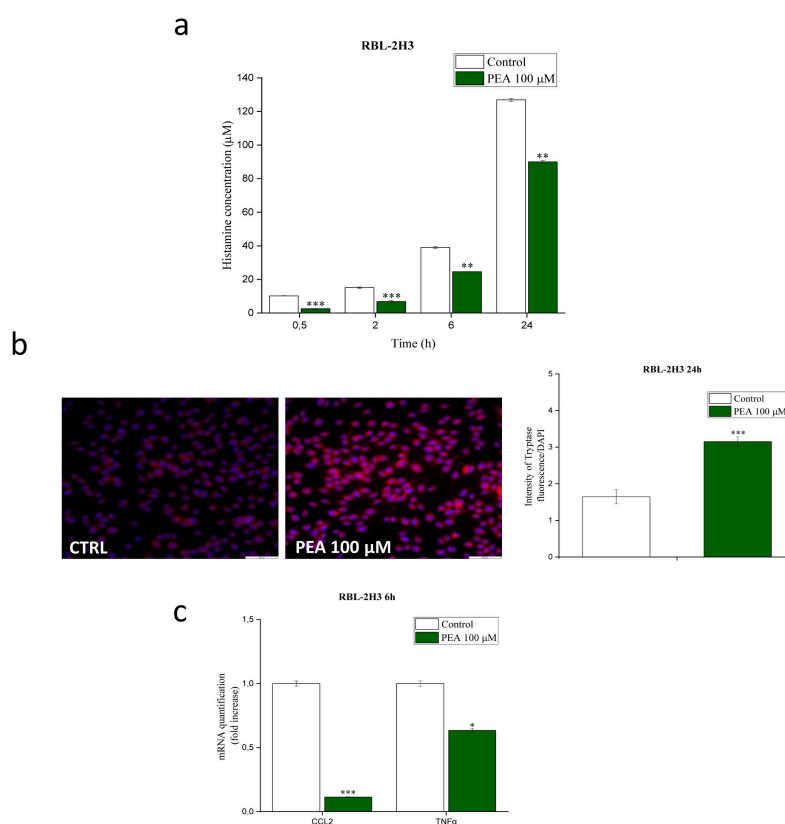


Figure 4. Long-lasting effect of PEA on MC degranulation. (a) Histamine concentration in the medium of RBL-2H3 cells pre-sensitized and pre-treated with PEA 100 μM for 18 h and stimulated with DNP-BSA the next day for 30 min, 2, 6 and 24 h. (b) Immunofluorescence of tryptase on RBL-2H3 cells pre-treated with PEA 100 μM for 18 h together with the pre-sensitization, and the next day stimulated with DNP-BSA for 24 h. Cell nuclei were labeled with DAPI. Scale bar = 50 μm . (c) RT-PCR of RBL-2H3 cells pre-sensitized and pre-treated with PEA 100 μM for 18 h and the next day stimulated with DNP-BSA for 6 h. DNP-BSA was used at a final concentration of 625 ng/mL in all experiments. Control condition was arbitrarily set at 1, values are expressed as the mean \pm S.E.M. of three experiments. * $p < 0.05$; ** $p < 0.01$; *** $p < 0.001$ vs. control.

3.5. PEA Down-Modulates Mast Cell-Induced Astrocyte Expression of Genes Involved in Inflammation and Pain

First, the effect of morphine and PEA on primary cortical astrocyte viability was evaluated as better detailed in the Supplementary section. Briefly, cell viability was not affected by increasing concentrations of morphine (1–30 μM) while PEA (10–30 μM) affected astrocyte viability, either used alone or in combination with morphine (Figure S5).

Second, the presence and functional expression of μ -receptors was studied, using western blot and calcium influx respectively, confirming that primary cortical astrocytes express a functional μ -receptor (Figure S6). The effect of RBL-2H3 cell mediators (with or without PEA treatment) on astrocyte viability and activity (with or without morphine treatment) was then studied by incubating the primary cortical astrocytes with RBL-2H3 cell medium. Briefly, we showed that RBL-2H3 cell-conditioned medium does not affect astrocytes viability (Figure 5a). Furthermore, by using RT-PCR we showed that morphine treatment does not alter the astrocyte expression of any of the investigated genes, i.e., GFAP, EAAT2, Serpina3n, IL-1 β , IL-6, CCL2. On the contrary, control astrocytes incubated with control RBL-2H3 cell medium showed a significant increase in the expression of all the genes but EAAT2 (Figure 5b,c). Cell medium from PEA pre-treated RBL-2H3 cells significantly reversed the increased expression for all the investigated genes, except GFAP that was furtherly increased (Figure 5b,c). The morphine-treated astrocytes incubated with control RBL-2H3 cell media showed a significant increase in the expression of all the genes examined, including EAAT2, with values exceeding those in control astrocytes treated with the same medium. The incubation with cell medium from PEA pre-treated RBL-2H3 cells significantly reversed the increased expression of all genes, except for GFAP (Figure 5b,c). In order to better understand the apparently contradictory findings on GFAP gene expression, immunofluorescence analysis of GFAP was performed. In contrast to RT-PCR findings, increased GFAP staining was observed in 30 μ M morphine-treated astrocytes. Similar findings were also seen in control (and even more so in morphine-treated astrocytes) incubated with control RBL-2H3 cell medium. In line with RT-PCR findings, the cell medium from PEA pre-treated RBL-2H3 cells further enhanced GFAP staining compared to control RBL-2H3 cell medium, both in control and morphine-treated astrocytes (Figure 6). Summarizing, morphine alone did not change the gene expression profile of astrocytes, while increasing GFAP immunoreactivity. On the contrary, a significant increase of the investigated genes was evident if mediators from RBL-2H3 cells were added. Finally, pre-treatment of RBL-2H3 cells with PEA significantly down-modulated the expression of astrocyte genes involved in neuropathic pain and inflammation.

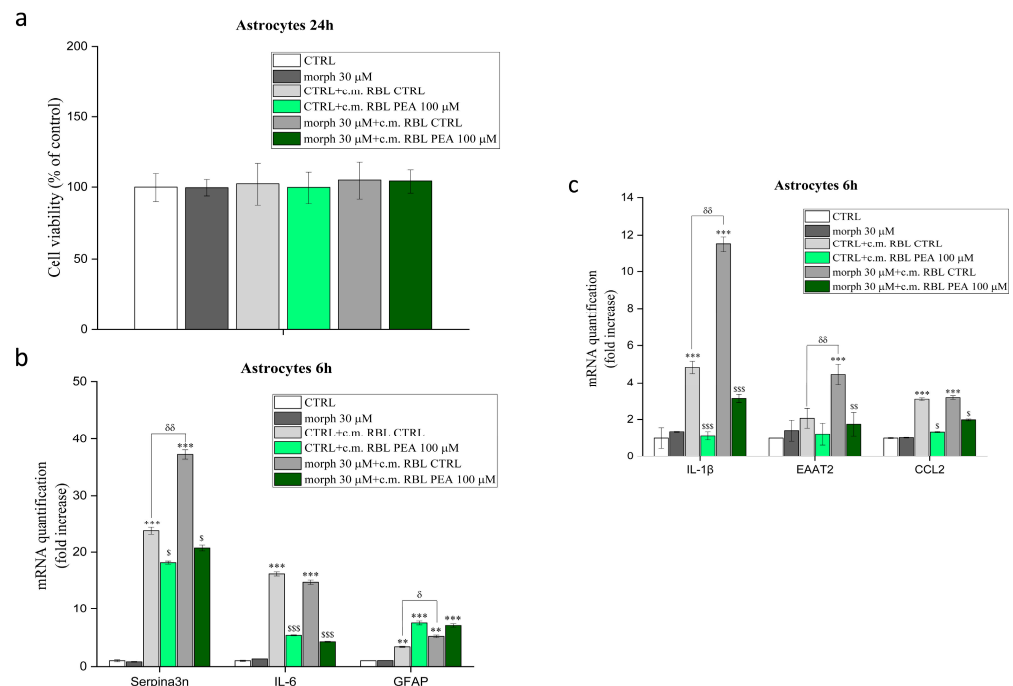


Figure 5. Effect of control and PEA pre-treated MC medium on astrocyte viability and gene expression. (a) MTT of astrocytes treated with 30 μ M morphine (48 h) and conditioned medium (c.m.) from RBL-2H3 (24 h) stimulated with DNP-BSA (24 h) and pre-treated or not (control) with 100 μ M PEA.

Control condition was arbitrarily set at 100, values are expressed as the mean \pm S.E.M. of two experiments. (b,c) RT-PCR of astrocytes treated with 30 μ M morphine (48 h) and conditioned medium (c.m.) from RBL-2H3 (6 h) stimulated with DNP-BSA (24 h) and pre-treated or not (control) with 100 μ M PEA. Control condition was arbitrarily set at 1, values are expressed as the mean \pm S.E.M. of three experiments. DNP-BSA was used at a final concentration of 625 ng/mL in all experiments. ** $p < 0.01$; *** $p < 0.001$ vs. control astrocytes. \$ $p < 0.05$; \$\$ $p < 0.01$; \$\$\$ $p < 0.001$ vs astrocytes + c.m. RBL-2H3 CTRL. δ $p < 0.05$; $\delta\delta$ $p < 0.01$ morphine astrocytes + c.m. RBL-2H3 CTRL vs. control astrocytes + c.m. RBL-2H3 CTRL.

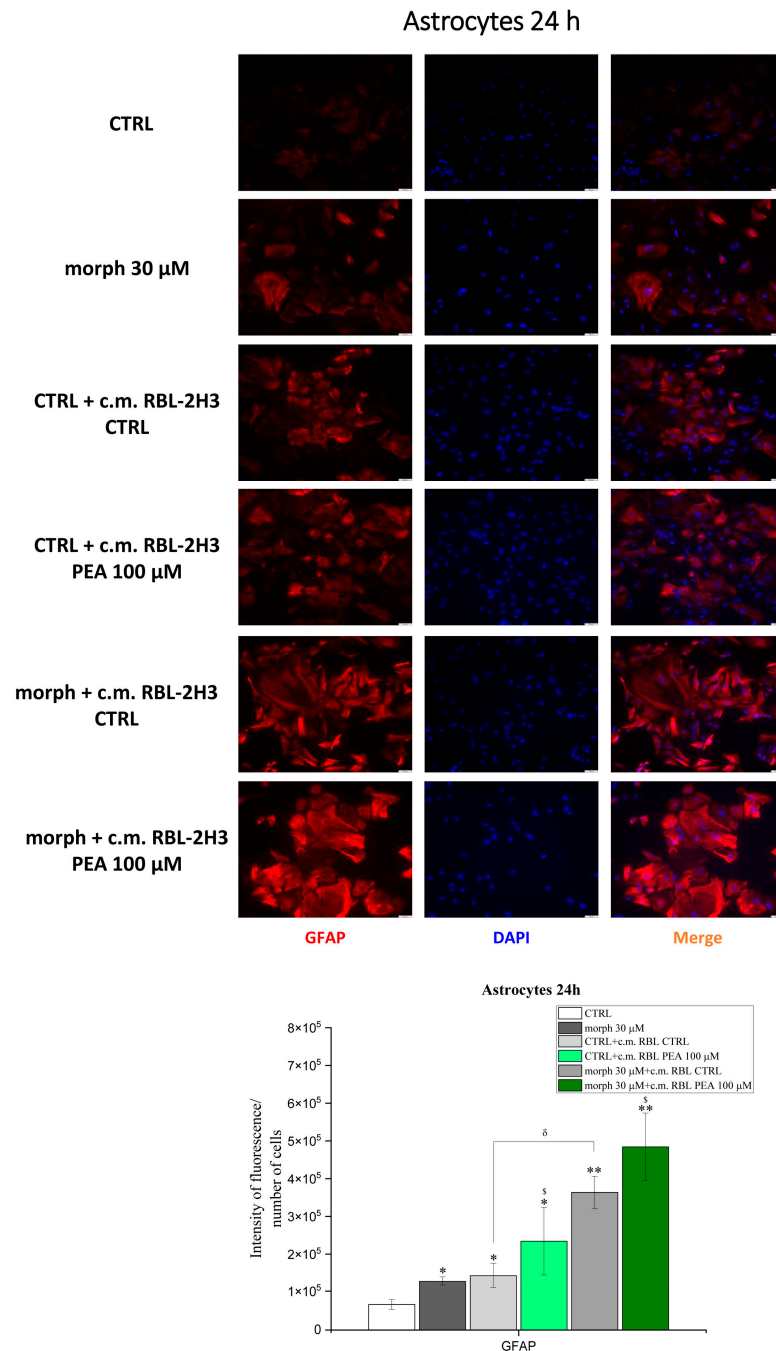


Figure 6. Effect of control and PEA pre-treated RBL-2H3 medium on astrocyte GFAP expression. Immunofluorescence of GFAP on astrocytes treated with 30 μ M morphine (48 h) and c.m. from RBL-2H3 (24 h) stimulated with DNP-BSA (625 ng/mL, 24 h) and pre-treated or not (control) with

100 μ M PEA. Cell nuclei were labeled with DAPI. Values are expressed as the mean \pm S.E.M. of three experiments. Scale bar = 50 μ m. * $p < 0.05$; ** $p < 0.01$ vs. control astrocytes. $^{\$}$ $p < 0.05$ vs. astrocytes + c.m. RBL-2H3 CTRL. $^{\delta}$ $p < 0.05$; morphine astrocytes + c.m. RBL-2H3 CTRL vs. control astrocytes + c.m. RBL-2H3 CTRL.

4. Discussion

The management of persistent pain is a major challenge for clinicians as well as patients. Opioids are the treatment of choice, but their use is limited by the occurrence of side effects such as tolerance. We have recently shown that ultramicrosized PEA effectively delays tolerance to morphine, tramadol and oxycodone [18,41]. Moreover, ultramicrosized PEA was shown to enhance the analgesic effect of opioids, thus limiting their dosage and side effects, both in naïve and neuropathic animals [48,49]. However, the mechanisms underlying the ability of PEA to reduce opioid tolerance are still unclear.

In light of the evidence that (i) PEA down-modulates MC degranulation [50] and (ii) glial cells are involved in the onset of tolerance [19], we hypothesized and proved that RBL-2H3 mediators activate astrocytes, while PEA counteracts this activation by down-modulating RBL-2H3 degranulation.

Mast cells are immune cells increasingly recognized to play pivotal roles not only in allergy, but also in host defense, innate and acquired immunity, homeostatic responses, [51] and inflammation [52]. Mast cells are located in almost all tissues, particularly around blood vessels and in proximity of nerve endings [52], with the same distribution being observed at meningeal level, both in the spinal cord and brain [53,54]. The critical role of MCs in the generation and maintenance of neuropathic pain has recently been investigated [55]. In particular, MC degranulated mediators, including nerve growth factor [56], have been shown to activate and sensitize nociceptors [57,58] as well as stimulate particular pain pathways [59].

Here we used a validated model of rat MCs, i.e., the RBL-2H3 cell line, and confirmed that sensitization with anti-dinitrophenyl (DNP)-IgE is needed to induce a tunable degranulation, as previously reported by other groups [47,60–62]. Although opioids, such as morphine, are known to activate MCs in vivo [61–64] and codeine was shown to induce human MC degranulation in vitro [65], the effect of morphine on the RBL-2H3 cell line was not investigated yet. Here we showed that morphine was able to significantly and dose-dependently increase degranulation of DNP-BSA-primed RBL-2H3 cells, without exerting any cytotoxic effect at the 0.3–300 μ M dose range. Interestingly, morphine-induced degranulation was not only monitored by the release of a well-known MC mediator, i.e., β -hexosaminidase [66], but also by immunofluorescence for tryptase, a serine protease stored in MC granules [67] and released upon MC activation [52,68]. Although the presence of tryptase in RBL-2H3 cells has been questioned [69], our finding is in line with previous studies confirming tryptase release in RBL-2H3 after appropriate stimulation [47,70].

Moreover, here we showed for the first time that RBL-2H3 cells express the μ -receptor. This is consistent with what has been previously shown in human MCs (both primary and cell line LAD2) [65]. Although the exact involvement of μ -receptors in morphine-induced MC degranulation was out of the scope of the present study and was not further investigated, it could be assumed that morphine effect depended on μ -receptors, even if alternative pathways were identified (e.g., Mas-related G protein-coupled receptor) [71].

In the present study, the ability of ultramicrosized PEA to down-modulate MC degranulation, in response to DNP-BSA challenge, either alone or associated with morphine, was confirmed. In particular, the effect of ultramicrosized PEA was monitored by β -hexosaminidase assay, tryptase immunofluorescence, histamine quantification and RT-PCR for newly synthesized mediators (i.e., CCL2 and TNF- α).

Within pre-formed granules, histamine is one of the main molecules produced by MCs [72], acting as a pro-inflammatory factor [73]. Our results demonstrated a time-

dependent histamine release in RBL-2H3 cells, counteracted by PEA treatment up to 24 h of DNP-BSA stimulation. The result parallels with that obtained by another group in which histamine was measured by ELISA assay [50]. Moreover, the ability of ultramicrosized PEA to decrease histamine levels was also observed by our group in a rat model of chronic neuropathic pain [49].

Notably, TNF- α may activate MCs as well as microglia and astrocytes, being involved in neuroinflammation and chronic pain [74], while CCL2 regulates recruitment of inflammatory cells [75] and acts as a chemoattractant to MCs [76]. The present results concerning the effect of PEA on RBL-2H3 are consistent with previous findings showing that this lipid amide negatively controls releasability of activated MCs, both in vitro [50,77,78], ex vivo [79] and in vivo [80,81], in accordance with the so-called ALIA mechanism originally postulated by the Nobel laureate Rita Levi Montalcini [82].

MCs can interact with virtually all cell populations in the CNS, particularly glial cells [53]. Interestingly, several lines of evidence indicate that chronic morphine treatment may directly or indirectly activate glial cells [13,19,83], resulting in the release of pro-inflammatory cytokines (such as TNF- α , IL-1 β , IL-6 and chemokines), which in turn further sensitize the NMDA receptors, promoting the onset of morphine tolerance [84]. In particular, astrocytes are emerging as relevant players in the development of opioid tolerance [19,85,86] and morphine repeated treatment was found to significantly activate astrocytes in the spinal horn [87]. Consistent with previous findings [88,89], we here showed that primary rat cortical astrocytes express the μ -receptor and release calcium in response to morphine, thus confirming previous findings on the astrocyte-activating effect of morphine [90]. Notably, the lack of morphine toxicity towards astrocytes was also shown.

The existence of a crosstalk between MCs and astrocyte in opioid tolerance development is an intriguing hypothesis that has not yet been evaluated. In the CNS, MCs are located at the meningeal [54] and blood brain barrier levels, in apposition to astrocytes and neurons and may enter the parenchyma when barrier permeability is increased [53,91]. Moreover, the powerful mediators released by MCs in the periphery can signal to the CNS compartment including astrocytes [92]. To study this relationship, morphine-activated cortical astrocytes were incubated with the conditioned medium of control or PEA pre-treated MCs. First, it was confirmed that MC medium did not alter astrocyte viability. Untreated MC medium led to a significant increase in gene expression of IL-1 β , IL-6, CCL2, Serpina3n, EAAT2 and GFAP, in control and even more so in morphine-treated astrocytes, thus confirming the involvement of these non-neuronal cells in neuroinflammation [84]. Interestingly, the increase in the expression of astrocyte neuroinflammatory (but not proliferative, i.e., GFAP) genes was effectively counteracted by pre-treatment of MCs with ultramicrosized PEA.

IL-1 β is one of the first cytokines that have been involved in the onset of morphine tolerance: selective blockade of the signaling associated with IL-1 β prevented the development of tolerance following chronic administration of morphine [93]. Moreover, once tolerance was established, intrathecal administration of an IL-1 receptor antagonist reversed hyperalgesia and prevented the additional development of tolerance and allodynia [53]. In addition, IL-1 β knockout mice showed an increased morphine analgesia and prevention of morphine tolerance [93]. Accordingly, the decrease of IL-1 β gene expression in response to incubation of morphine-treated astrocytes with PEA-treated MC medium might be considered as a protective effect of PEA against opioid-associated neuroinflammation.

IL-6, whose production is induced by IL-1 β and TNF- α , is also involved in morphine tolerance, as well as TNF- α itself, whose inhibition suppress the development of morphine tolerance in rats [94]. High levels of spinal IL-6 have been shown in tolerant rats [95] and repeated intrathecal administration of melanocortin 4 receptor antagonist reduced IL-6 expression and decreased astrocyte activation in morphine tolerant rats, counteracting the loss of morphine analgesic effect [96]. The decreased astrocytic gene expression of IL-6 in response to PEA-treated MC medium might again confirm the protective effect

of PEA against neuroinflammation. As far as the chemokine CCL2 concerns, similar considerations could be drawn. Indeed, CCL2 is up-regulated during neuropathic pain conditions, while its neutralization (through intrathecal antibodies) improved morphine-induced analgesia [97].

Beside inflammatory cytokines and chemokines, other markers of astrocyte activation were analyzed here, to evaluate astrocyte phenotype and functions. SERPINA3 is an acute phase protein [98] belonging to the serpin superfamily of serine protease inhibitors [99]. SERPINA3 is synthesized mainly in the liver, lungs, and brain [100]. Here, activated astrocytes represent the main producers of SERPINA3 [101], whose expression is increased in response to IL-1 and TNF- α [102]. Previous experiments have shown that mice lacking *serpina3n* gene develop a more severe mechanical allodynia compared to wild-type mice [103]. Interestingly, *Serpina3n* was found to be upregulated in postmortem mid brain tissues from chronic cocaine abusers [104], and the astrogliosis induced by ischemic stroke-associated neuroinflammation was characterized by increased *Serpina3n* mRNA expression [105]. Furthermore, *Serpina3n* is involved in neuropathic pain [103] and was actually found to be upregulated in dorsal root ganglia after peripheral nerve injury [106]. With this in mind, the down-regulation of *Serpina3n* expression in morphine-treated astrocytes following incubation with the medium of PEA-treated MCs can be considered a further proof of the ability of ultramicrosized PEA to rebalance the astrocyte-MC crosstalk. A possible explanation for this finding could be that ultramicrosized PEA downmodulated TNF- α release from MCs, with this cytokine being responsible for the onset of morphine tolerance in vivo [94]. The hypothesis is supported by the in vivo evidence that TNF- α levels are lower in rats co-treated with morphine and PEA compared to those treated with morphine only [18].

Excitatory amino acid transporter 2 (EAAT2) is primarily localized on astrocytes and responsible for up to 90% of glutamate uptake in the brain [107]. Some evidence correlates a down-regulation of EAAT2 to chronic morphine treatment and pain-related conditions, although a defined role of this transporter is still unclear. In our experiments, EAAT2 over-expression on astrocytes may be viewed as an attempt to enhance glutamate up-take during neuroinflammation.

Finally, the up-regulation of GFAP, i.e., the main intermediate filament protein of the astrocyte cytoskeletal compartment [108], is a key feature of astrocyte activation [108] responsible for both pathogenetic and protective roles [109,110]. While in vivo studies have mainly shown GFAP up-regulation in response to morphine chronic treatment [18,19,111], in vitro findings have been more inconsistent. In the present study, an up-regulation of GFAP in morphine-treated astrocytes was observed, with MC conditioned medium further increasing its expression. Surprisingly, the incubation of astrocytes with the conditioned medium from PEA-treated MCs resulted in an opposite effect on the expression of GFAP (i.e., increase) compared to all the other investigated genes, which indeed were decreased. In the light of the observed down-regulation of inflammatory genes, it might be inferred that in the evaluated in vitro system, GFAP increase in astrocytes is part of the PEA-mediated protective response to morphine potential damage.

5. Conclusions

In conclusion, the present study showed that morphine-induced MC degranulation leads to astrocyte activation, with MC mediators inducing astrocyte over-expression of genes involved in pain and inflammation. Pre-treatment with ultramicrosized PEA decreased MC degranulation and reduced the expression of these astrocyte genes accordingly. Given the known involvement of astrocytes in the development and maintenance of morphine tolerance, our findings highlight one of the pathways through which PEA may control this phenomenon, balancing the crosstalk between MCs and astrocytes. This research lays the foundations for a more in-depth study on the molecular mechanisms sustaining PEA-induced MC down-regulation and modulation of glial cell behavior.

Supplementary Materials: The following supporting information can be downloaded at: <https://www.mdpi.com/article/10.3390/biom13020233/s1>, Tables S1. Chromatographic gradient with valve position switch time. Tables S2. MRM parameters. Tables S3. Linear regression coefficients and LOD. Tables S4. Accuracy & Precision (RSD) values for histamine. Tables S5. ME & RE values for histamine. Figure S1. The injection valve position in 2D-HPLC system. Figure S2. Entire Western blot of MOR-1 in RBL-2H3. Figure S3. Optimization of RBL-2H3 degranulation protocol. Figure S4. Effect of PEA 10 and 100 μ M on RBL-2H3 degranulation. Figure S5. Effect of morphine and PEA on astrocyte viability. Figure S6. Effect of morphine on astrocyte calcium release [112–114].

Author Contributions: Conceptualization, C.G. (Carla Ghelardini) and L.D.C.M.; methodology, A.T., V.F., G.B. and M.P.; software, F.M. and P.F.; validation, C.C. and L.M.; formal analysis, C.C.; investigation, A.T. and E.L.; resources, L.M. and C.G. (Chiara Gomiero); data curation, A.T. and E.L.; writing—original draft preparation, A.T. and C.G. (Chiara Gomiero); writing—review and editing, A.T. and L.D.C.M.; visualization, P.F.; supervision, C.G. (Carla Ghelardini); project administration, C.G. (Carla Ghelardini); funding acquisition, L.D.C.M. and C.G. (Carla Ghelardini). All authors have read and agreed to the published version of the manuscript.

Funding: This research was supported by the Italian Ministry of University and Research and by the University of Florence.

Institutional Review Board Statement: The study was conducted according to ARRIVE guidelines and approved by the Animal Subjects Review Board of the University of Florence and by the Italian Ministry of Health (No. 498/2017-PR).

Informed Consent Statement: Not applicable.

Data Availability Statement: The data presented in this study are available on request from the corresponding author.

Conflicts of Interest: C.G. (Chiara Gomiero) discloses a contract with Epitech Group SpA, which had no role in study design and execution, data analysis and interpretation, in the writing of the report, and in the decision to submit the paper for publication. The remaining authors declare no conflict of interest.

References

1. Gatchel, R.J.; McGeary, D.D.; McGeary, C.A.; Lippe, B. Interdisciplinary Chronic Pain Management: Past, Present, and Future. *Am. Psychol.* **2014**, *69*, 119–130. [[CrossRef](#)] [[PubMed](#)]
2. Yaksh, T.L. Pain after Injury: Some Basic Mechanisms. *J. Fla. Med. Assoc.* **1997**, *84*, 16–19.
3. White, P.F.; Kehlet, H. Improving Postoperative Pain Management: What Are the Unresolved Issues? *Anesthesiology* **2010**, *112*, 220–225. [[CrossRef](#)]
4. Sierra-Silvestre, E.; Somerville, M.; Bisset, L.; Coppieters, M.W. Altered Pain Processing in Patients with Type 1 and 2 Diabetes: Systematic Review and Meta-Analysis of Pain Detection Thresholds and Pain Modulation Mechanisms. *BMJ Open Diabetes Res. Care* **2020**, *8*, e001566. [[CrossRef](#)] [[PubMed](#)]
5. Dieppe, P.A.; Lohmander, L.S. Pathogenesis and Management of Pain in Osteoarthritis. *Lancet* **2005**, *365*, 965–973. [[CrossRef](#)]
6. Portenoy, R.K.; Ahmed, E. Cancer Pain Syndromes. *Hematol. Oncol. Clin. N. Am.* **2018**, *32*, 371–386. [[CrossRef](#)]
7. Farquhar-Smith, P. Chemotherapy-Induced Neuropathic Pain. *Curr. Opin. Support. Palliat. Care* **2011**, *5*, 1–7. [[CrossRef](#)]
8. Shaheed, C.A.; Machado, G.C.; Underwood, M. Drugs for Chronic Pain. *Br. J. Gen. Pract.* **2020**, *70*, 576–577. [[CrossRef](#)]
9. Haghjooy-Javanmard, S.; Ghasemi, A.; Laher, I.; Zarrin, B.; Dana, N.; Vaseghi, G. Influence of Morphine on TLR4/NF-KB Signaling Pathway of MCF-7 Cells. *Bratisl. Lek. Listy* **2018**, *119*, 229–233. [[CrossRef](#)]
10. Ghelardini, C.; Di Cesare Mannelli, L.; Bianchi, E. The Pharmacological Basis of Opioids. *Clin. Cases Miner. Bone Metab.* **2015**, *12*, 219–221. [[CrossRef](#)]
11. Vanegas, G.; Ripamonti, C.; Sbanotto, A.; de Conno, F. Side Effects of Morphine Administration in Cancer Patients. *Cancer Nurs.* **1998**, *21*, 289–297. [[CrossRef](#)] [[PubMed](#)]
12. Dumas, E.O.; Pollack, G.M. Opioid Tolerance Development: A Pharmacokinetic/Pharmacodynamic Perspective. *AAPS J.* **2008**, *10*, 537–551. [[CrossRef](#)] [[PubMed](#)]
13. Mika, J.; Wawrzczak-Bargiela, A.; Osikowicz, M.; Makuch, W.; Przewlocka, B. Attenuation of Morphine Tolerance by Minocycline and Pentoxifylline in Naive and Neuropathic Mice. *Brain Behav. Immun.* **2009**, *23*, 75–84. [[CrossRef](#)]
14. Davis, M. Modulation of Microglia Can Attenuate Neuropathic Pain Symptoms and Enhance Morphine Effectiveness. *J. Pain Palliat. Care Pharmacother.* **2009**, *23*.
15. Mahmoud, S.; Gharagozloo, M.; Simard, C.; Gris, D. Astrocytes Maintain Glutamate Homeostasis in the CNS by Controlling the Balance between Glutamate Uptake and Release. *Cells* **2019**, *8*, 184. [[CrossRef](#)]

16. Blanco-Suárez, E.; Caldwell, A.L.M.; Allen, N.J. Role of Astrocyte-Synapse Interactions in CNS Disorders. *J. Physiol.* **2017**, *595*, 1903–1916. [[CrossRef](#)]
17. Duran, J.; Gruart, A.; López-Ramos, J.C.; Delgado-García, J.M.; Guinovart, J.J. Glycogen in Astrocytes and Neurons: Physiological and Pathological Aspects. *Adv. Neurobiol.* **2019**, *23*, 311–329. [[CrossRef](#)] [[PubMed](#)]
18. Di Cesare Mannelli, L.; Corti, F.; Micheli, L.; Zanardelli, M.; Ghelardini, C. Delay of Morphine Tolerance by Palmitoylethanolamide. *Biomed. Res. Int.* **2015**, *2015*, 894732. [[CrossRef](#)]
19. Song, P.; Zhao, Z.Q. The Involvement of Glial Cells in the Development of Morphine Tolerance. *Neurosci. Res.* **2001**, *39*, 281–286. [[CrossRef](#)]
20. Mika, J.; Osikowicz, M.; Makuch, W.; Przewlocka, B. Minocycline and Pentoxifylline Attenuate Allodynia and Hyperalgesia and Potentiate the Effects of Morphine in Rat and Mouse Models of Neuropathic Pain. *Eur. J. Pharmacol.* **2007**, *560*, 142–149. [[CrossRef](#)]
21. Cui, Y.; Liao, X.X.; Liu, W.; Guo, R.X.; Wu, Z.Z.; Zhao, C.M.; Chen, P.X.; Feng, J.Q. A Novel Role of Minocycline: Attenuating Morphine Antinociceptive Tolerance by Inhibition of P38 MAPK in the Activated Spinal Microglia. *Brain Behav. Immun.* **2008**, *22*, 114–123. [[CrossRef](#)]
22. Raghavendra, V.; Tanga, F.Y.; DeLeo, J.A. Attenuation of Morphine Tolerance, Withdrawal-Induced Hyperalgesia, and Associated Spinal Inflammatory Immune Responses by Propentofylline in Rats. *Neuropsychopharmacology* **2003**, *29*, 327–334. [[CrossRef](#)]
23. D'aloia, A.; Molteni, L.; Gullo, F.; Bresciani, E.; Artusa, V.; Rizzi, L.; Ceriani, M.; Meanti, R.; Lecchi, M.; Coco, S.; et al. Palmitoylethanolamide Modulation of Microglia Activation: Characterization of Mechanisms of Action and Implication for Its Neuroprotective Effects. *Int. J. Mol. Sci.* **2021**, *22*, 3054. [[CrossRef](#)] [[PubMed](#)]
24. Re, G.; Barbero, R.; Miolo, A.; di Marzo, V. Palmitoylethanolamide, Endocannabinoids and Related Cannabimimetic Compounds in Protection against Tissue Inflammation and Pain: Potential Use in Companion Animals. *Vet. J.* **2007**, *173*, 21–30. [[CrossRef](#)] [[PubMed](#)]
25. Beggiato, S.; Tomasini, M.C.; Ferraro, L. Palmitoylethanolamide (PEA) as a Potential Therapeutic Agent in Alzheimer's Disease. *Front. Pharmacol.* **2019**, *10*, 821. [[CrossRef](#)] [[PubMed](#)]
26. Gabrielsson, L.; Mattsson, S.; Fowler, C.J. Palmitoylethanolamide for the Treatment of Pain: Pharmacokinetics, Safety and Efficacy. *Br. J. Clin. Pharmacol.* **2016**, *82*, 932–942. [[CrossRef](#)]
27. Artukoglu, B.B.; Beyer, C.; Zulloff-Shani, A.; Brener, E.; Bloch, M.H. Efficacy of Palmitoylethanolamide for Pain: A Meta-Analysis. *Pain Physician* **2017**, *20*, 353.
28. Rankin, L.; Fowler, C.J. The Basal Pharmacology of Palmitoylethanolamide. *Int. J. Mol. Sci.* **2020**, *21*, 7942. [[CrossRef](#)]
29. Gabrielsson, L.; Gouveia-Figueira, S.; Häggström, J.; Alhouayek, M.; Fowler, C.J. The Anti-Inflammatory Compound Palmitoylethanolamide Inhibits Prostaglandin and Hydroxyeicosatetraenoic Acid Production by a Macrophage Cell Line. *Pharmacol. Res. Perspect.* **2017**, *5*, e00300. [[CrossRef](#)]
30. Di Cesare Mannelli, L.; D'Agostino, G.; Pacini, A.; Russo, R.; Zanardelli, M.; Ghelardini, C.; Calignano, A. Palmitoylethanolamide Is a Disease-Modifying Agent in Peripheral Neuropathy: Pain Relief and Neuroprotection Share a PPAR-Alpha-Mediated Mechanism. *Mediat. Inflamm.* **2013**, *2013*, 328797. [[CrossRef](#)]
31. Nguyen, J.; Luk, K.; Vang, D.; Soto, W.; Vincent, L.; Robiner, S.; Saavedra, R.; Li, Y.; Gupta, P.; Gupta, K. Morphine Stimulates Cancer Progression and Mast Cell Activation and Impairs Survival in Transgenic Mice with Breast Cancer. *Br. J. Anaesth.* **2014**, *113* (Suppl. 1), i4–i13. [[CrossRef](#)]
32. Grosman, N. Histamine Release from Isolated Rat Mast Cells: Effect of Morphine and Related Drugs and Their Interaction with Compound 48/80. *Agents Actions* **1981**, *11*, 196–203. [[CrossRef](#)]
33. Vincent, L.; Vang, D.; Nguyen, J.; Gupta, M.; Luk, K.; Ericson, M.E.; Simone, D.A.; Gupta, K. Mast Cell Activation Contributes to Sickle Cell Pathobiology and Pain in Mice. *Blood* **2013**, *122*, 1853–1862. [[CrossRef](#)]
34. Mazzari, S.; Canella, R.; Petrelli, L.; Marcolongo, G.; Leon, A. N-(2-Hydroxyethyl) Hexadecanamide Is Orally Active in Reducing Edema Formation and Inflammatory Hyperalgesia by down-Modulating Mast Cell Activation. *Eur. J. Pharmacol.* **1996**, *300*, 227–236. [[CrossRef](#)]
35. Beggiato, S.; Borelli, A.C.; Ferraro, L.; Tanganelli, S.; Antonelli, T.; Tomasini, M.C. Palmitoylethanolamide Blunts Amyloid-B42-Induced Astrocyte Activation and Improves Neuronal Survival in Primary Mouse Cortical Astrocyte-Neuron Co-Cultures. *J. Alzheimer's Dis.* **2018**, *61*, 389–399. [[CrossRef](#)] [[PubMed](#)]
36. Blank, U.; Varin-Blank, N. La Lignée Mastocytaire RBL: Modèle Expérimental in Vitro et Application En Pharmacologie Clinique. *Rev. Fr. Allergol. Immunol. Clin.* **2004**, *44*, 51–56. [[CrossRef](#)]
37. McCarthy, K.D.; de Vellis, J. Preparation of Separate Astroglial and Oligodendroglial Cell Cultures from Rat Cerebral Tissue. *J. Cell Biol.* **1980**, *85*, 890–902. [[CrossRef](#)] [[PubMed](#)]
38. Berridge, M.V.; Tan, A.S. Characterization of the Cellular Reduction of 3-(4,5-Dimethylthiazol-2-Yl)-2,5-Diphenyltetrazolium Bromide (MTT): Subcellular Localization, Substrate Dependence, and Involvement of Mitochondrial Electron Transport in MTT Reduction. *Arch. Biochem. Biophys.* **1993**, *303*, 474–482. [[CrossRef](#)]
39. Jönsson, D.; Nilsson, B.O. The Antimicrobial Peptide LL-37 Is Anti-Inflammatory and Proapoptotic in Human Periodontal Ligament Cells. *J. Periodontal Res.* **2012**, *47*, 330–335. [[CrossRef](#)]
40. Kawahara, T. Establishment and Characterization of Mouse Bone Marrow-Derived Mast Cell Hybridomas. *Exp. Cell Res.* **2012**, *318*, 2385–2396. [[CrossRef](#)]

41. Micheli, L.; Lucarini, E.; Toti, A.; Ferrara, V.; Ciampi, C.; Parisio, C.; Bartolucci, G.; Mannelli, L.D.C.; Ghelardini, C. Effects of Ultramicrosized N-Palmitoylethanolamine Supplementation on Tramadol and Oxycodone Analgesia and Tolerance Prevention. *Pharmaceutics* **2022**, *14*, 403. [[CrossRef](#)] [[PubMed](#)]
42. Micheli, L.; Parisio, C.; Lucarini, E.; Vona, A.; Toti, A.; Pacini, A.; Mello, T.; Boccella, S.; Ricciardi, F.; Maione, S.; et al. VEGF-A/VEGFR-1 Signalling and Chemotherapy-Induced Neuropathic Pain: Therapeutic Potential of a Novel Anti-VEGFR-1 Monoclonal Antibody. *J. Exp. Clin. Cancer Res.* **2021**, *40*, 320. [[CrossRef](#)] [[PubMed](#)]
43. Nistri, S.; Mannelli, L.D.C.; Ghelardini, C.; Zanardelli, M.; Bani, D.; Failli, P. Pretreatment with Relaxin Does Not Restore NO-Mediated Modulation of Calcium Signal in Coronary Endothelial Cells Isolated from Spontaneously Hypertensive Rats. *Molecules* **2015**, *20*, 9524–9535. [[CrossRef](#)]
44. Passante, E.; Ehrhardt, C.; Sheridan, H.; Frankish, N. RBL-2H3 Cells Are an Imprecise Model for Mast Cell Mediator Release. *Inflamm. Res.* **2009**, *58*, 611–618. [[CrossRef](#)] [[PubMed](#)]
45. Passante, E.; Frankish, N. The RBL-2H3 Cell Line: Its Provenance and Suitability as a Model for the Mast Cell. *Inflamm. Res.* **2009**, *58*, 737–745. [[CrossRef](#)] [[PubMed](#)]
46. Qian, F.; Guo, G.; Li, Y.; Kulka, M. A Novel Eremophilane Lactone Inhibits FcεRI-Dependent Release of pro-Inflammatory Mediators: Structure-Dependent Bioactivity. *Inflamm. Res.* **2016**, *65*, 303–311. [[CrossRef](#)]
47. Rujitharanawong, C.; Yoodee, S.; Sueksakit, K.; Peerapen, P.; Tuchinda, P.; Kulthanan, K.; Thongboonkerd, V. Systematic Comparisons of Various Markers for Mast Cell Activation in RBL-2H3 Cells. *Cell Tissue Res.* **2022**, *390*, 413–428. [[CrossRef](#)]
48. Di Cesare Mannelli, L.; Micheli, L.; Lucarini, E.; Ghelardini, C. N-Palmitoylethanolamine Supplementation for Long-Lasting, Low-Dosed Morphine Antinociception. *Front. Pharmacol.* **2018**, *9*, 473. [[CrossRef](#)]
49. Micheli, L.; Lucarini, E.; Nobili, S.; Bartolucci, G.; Pallecchi, A.; Toti, A.; Ferrara, V.; Ciampi, C.; Ghelardini, C.; Di Cesare Mannelli, L. Ultramicrosized N-Palmitoylethanolamine Contributes to Morphine Efficacy against Neuropathic Pain: Implication of Mast Cells and Glia. *Curr. Neuropharmacol.* **2022**, *21*. [[CrossRef](#)]
50. Petrosino, S.; Schiano Moriello, A.; Verde, R.; Allarà, M.; Imperatore, R.; Ligresti, A.; Mahmoud, A.M.; Peritore, A.F.; Iannotti, F.A.; di Marzo, V. Palmitoylethanolamide Counteracts Substance P-Induced Mast Cell Activation in Vitro by Stimulating Diacylglycerol Lipase Activity. *J. Neuroinflamm.* **2019**, *16*, 274. [[CrossRef](#)]
51. Moon, T.C.; Dean Befus, A.; Kulka, M. Mast Cell Mediators: Their Differential Release and the Secretory Pathways Involved. *Front. Immunol.* **2014**, *5*, 569. [[CrossRef](#)]
52. Payne, V.; Kam, P.C.A. Mast Cell Tryptase: A Review of Its Physiology and Clinical Significance. *Anaesthesia* **2004**, *59*, 695–703. [[CrossRef](#)]
53. Mittal, A.; Sagi, V.; Gupta, M.; Gupta, K. Mast Cell Neural Interactions in Health and Disease. *Front. Cell. Neurosci.* **2019**, *13*, 110. [[CrossRef](#)]
54. Sayed, B.A.; Christy, A.L.; Walker, M.E.; Brown, M.A. Meningeal Mast Cells Affect Early T Cell Central Nervous System Infiltration and Blood-Brain Barrier Integrity through TNF: A Role for Neutrophil Recruitment? *J. Immunol.* **2010**, *184*, 6891–6900. [[CrossRef](#)] [[PubMed](#)]
55. Kaur, G.; Singh, N.; Jaggi, A.S. Mast Cells in Neuropathic Pain: An Increasing Spectrum of Their Involvement in Pathophysiology. *Rev. Neurosci.* **2017**, *28*, 759–766. [[CrossRef](#)] [[PubMed](#)]
56. Koda, H.; Mizumura, K. Sensitization to Mechanical Stimulation by Inflammatory Mediators and by Mild Burn in Canine Visceral Nociceptors in Vitro. *J. Neurophysiol.* **2002**, *87*, 2043–2051. [[CrossRef](#)] [[PubMed](#)]
57. Skaper, S.D.; Facci, L.; Giusti, P. Mast Cells, Glia and Neuroinflammation: Partners in Crime? *Immunology* **2014**, *141*, 314–327. [[CrossRef](#)] [[PubMed](#)]
58. Xanthos, D.N.; Gaderer, S.; Drdla, R.; Nuro, E.; Abramova, A.; Ellmeier, W.; Sandkühler, J. Central Nervous System Mast Cells in Peripheral Inflammatory Nociception. *Mol. Pain* **2011**, *7*, 1744–8069. [[CrossRef](#)] [[PubMed](#)]
59. Levy, D.; Kainz, V.; Burstein, R.; Strassman, A.M. Mast Cell Degranulation Distinctly Activates Trigemino-Cervical and Lumbosacral Pain Pathways and Elicits Widespread Tactile Pain Hypersensitivity. *Brain Behav. Immun.* **2012**, *26*, 311–317. [[CrossRef](#)]
60. Lian, Q.; Cheng, Y.; Zhong, C.; Wang, F. Inhibition of the IgE-Mediated Activation of RBL-2H3 Cells by TIPP, a Novel Thymic Immunosuppressive Pentapeptide. *Int. J. Mol. Sci.* **2015**, *16*, 2252. [[CrossRef](#)]
61. Fu, H.; Cheng, H.; Cao, G.; Zhang, X.; Tu, J.; Sun, M.; Mou, X.; Shou, Q.; Ke, Y. The Inhibition of Mast Cell Activation of Radix Paeoniae Alba Extraction Identified by TCRP Based and Conventional Cell Function Assay Systems. *PLoS ONE* **2016**, *11*, e0155930. [[CrossRef](#)] [[PubMed](#)]
62. Okahashi, N.; Nakata, M.; Hirose, Y.; Morisaki, H.; Kataoka, H.; Kuwata, H.; Kawabata, S. Streptococcal H₂O₂ Inhibits IgE-Triggered Degranulation of RBL-2H3 Mast Cell/Basophil Cell Line by Inducing Cell Death. *PLoS ONE* **2020**, *15*, e0231101. [[CrossRef](#)]
63. Yaksh, T.L.; Allen, J.W.; Veasart, S.L.; Horais, K.A.; Malkmus, S.A.; Scadeng, M.; Steinauer, J.J.; Rossi, S.S. Role of Meningeal Mast Cells in Intrathecal Morphine-Evoked Granuloma Formation. *Anesthesiology* **2013**, *118*, 664–678. [[CrossRef](#)] [[PubMed](#)]
64. Dybendal, T.; Guttormsen, A.B.; Elsayed, S.; Askeland, B.; Harboe, T.; Florvaag, E. Screening for Mast Cell Tryptase and Serum IgE Antibodies in 18 Patients with Anaphylactic Shock during General Anaesthesia. *Acta Anaesthesiol. Scand.* **2003**, *47*, 1211–1218. [[CrossRef](#)]
65. Sheen, C.H.; Schleimer, R.P.; Kulka, M. Codeine Induces Human Mast Cell Chemokine and Cytokine Production: Involvement of G-Protein Activation. *Allergy* **2007**, *62*, 532–538. [[CrossRef](#)]

66. Fukuishi, N.; Murakami, S.; Ohno, A.; Yamanaka, N.; Matsui, N.; Fukutsuji, K.; Yamada, S.; Itoh, K.; Akagi, M. Does β -Hexosaminidase Function Only as a Degranulation Indicator in Mast Cells? The Primary Role of β -Hexosaminidase in Mast Cell Granules. *J. Immunol.* **2014**, *193*, 1886–1894. [[CrossRef](#)] [[PubMed](#)]
67. Alanazi, S.; Grujic, M.; Lampinen, M.; Rollman, O.; Sommerhoff, C.P.; Pejler, G.; Melo, F.R. Mast Cell β -Tryptase Is Enzymatically Stabilized by DNA. *Int. J. Mol. Sci.* **2020**, *21*, 5065. [[CrossRef](#)] [[PubMed](#)]
68. Atiakshin, D.; Buchwalow, I.; Samoilova, V.; Tiemann, M. Tryptase as a Polyfunctional Component of Mast Cells. *Histochem. Cell Biol.* **2018**, *149*, 461–477. [[CrossRef](#)]
69. Shim, J.K.; Kennedy, R.H.; Weatherly, L.M.; Abovian, A.V.; Hashmi, H.N.; Rajaei, A.; Gosse, J.A. Searching for Tryptase in the RBL-2H3 Mast Cell Model: Preparation for Comparative Mast Cell Toxicology Studies with Zebrafish. *J. Appl. Toxicol.* **2019**, *39*, 473–484. [[CrossRef](#)]
70. Li, Y.; Sun, X.; Juan, Z.; Guan, X.; Wang, M.; Meng, Y.; Ma, R. Propofol Pretreatment Alleviates Mast Cell Degranulation by Inhibiting SOC to Protect the Myocardium from Ischemia–Reperfusion Injury. *Biomed. Pharmacother.* **2022**, *150*, 113014. [[CrossRef](#)]
71. Yaksh, T.L.; Eddinger, K.A.; Kokubu, S.; Wang, Z.; Dinardo, A.; Ramachandran, R.; Zhu, Y.; He, Y.; Weren, F.; Quang, D.; et al. Mast Cell Degranulation and Fibroblast Activation in the Morphine-Induced Spinal Mass: Role of Mas-Related G Protein-Coupled Receptor Signaling. *Anesthesiology* **2019**, *131*, 132–147. [[CrossRef](#)] [[PubMed](#)]
72. Thangam, E.B.; Jemima, E.A.; Singh, H.; Baig, M.S.; Khan, M.; Mathias, C.B.; Church, M.K.; Saluja, R. The Role of Histamine and Histamine Receptors in Mast Cell-Mediated Allergy and Inflammation: The Hunt for New Therapeutic Targets. *Front. Immunol.* **2018**, *9*, 1873. [[CrossRef](#)] [[PubMed](#)]
73. Carlos, D.; Sá-Nunes, A.; de Paula, L.; Matias-Peres, C.; Jamur, M.C.; Oliver, C.; Serra, M.F.; Martins, M.A.; Faccioli, L.H. Histamine Modulates Mast Cell Degranulation through an Indirect Mechanism in a Model IgE-Mediated Reaction. *Eur. J. Immunol.* **2006**, *36*, 1494–1503. [[CrossRef](#)]
74. Gu, Y.; Yang, D.K.; Spinas, E.; Kritas, S.K.; Saggini, A.; Caraffa, A.; Antinolfi, P.; Saggini, R.; Conti, P. Role of TNF in Mast Cell Neuroinflammation and Pain. *J. Biol. Regul. Homeost. Agents* **2015**, *29*, 787–791.
75. Castellani, M.L.; Bhattacharya, K.; Tagen, M.; Kempuraj, D.; Perrella, A.; de Lutiis, M.; Boucher, W.; Conti, P.; Theoharides, T.C.; Cerulli, G.; et al. Anti-Chemokine Therapy for Inflammatory Diseases. *Int. J. Immunopathol. Pharmacol.* **2016**, *20*, 447–453. [[CrossRef](#)]
76. Bischoff, S.C.; Krieger, M.; Brunner, T.; Rot, A.; Tschärner, V.V.; Baggiolini, M.; Dahinden, C.A. RANTES and Related Chemokines Activate Human Basophil Granulocytes through Different G Protein-coupled Receptors. *Eur. J. Immunol.* **1993**, *23*, 761–767. [[CrossRef](#)] [[PubMed](#)]
77. Facci, L.; Dal Toso, R.; Romanello, S.; Buriani, A.; Skaper, S.D.; Leon, A. Mast Cells Express a Peripheral Cannabinoid Receptor with Differential Sensitivity to Anandamide and Palmitoylethanolamide. *Proc. Natl. Acad. Sci. USA* **1995**, *92*, 3376–3380. [[CrossRef](#)]
78. Cerrato, S.; Brazis, P.; della Valle, M.F.; Miolo, A.; Puigdemont, A. Effects of Palmitoylethanolamide on Immunologically Induced Histamine, PGD₂ and TNF α Release from Canine Skin Mast Cells. *Vet. Immunol. Immunopathol.* **2010**, *133*, 9–15. [[CrossRef](#)] [[PubMed](#)]
79. Abramo, F.; Lazzarini, G.; Pirone, A.; Lenzi, C.; Albertini, S.; della Valle, M.F.; Schievano, C.; Vannozzi, I.; Miragliotta, V. Ultramicrosized Palmitoylethanolamide Counteracts the Effects of Compound 48/80 in a Canine Skin Organ Culture Model. *Vet. Dermatol.* **2017**, *28*, 104–456. [[CrossRef](#)]
80. Bettoni, I.; Comelli, F.; Colombo, A.; Bonfanti, P.; Costa, B. Non-Neuronal Cell Modulation Relieves Neuropathic Pain: Efficacy of the Endogenous Lipid Palmitoylethanolamide. *CNS Neurol. Disord. Drug Targets* **2013**, *12*, 34–44. [[CrossRef](#)]
81. Scarampella, F.; Abramo, F.; Noli, C. Clinical and Histological Evaluation of an Analogue of Palmitoylethanolamide, PLR 120 (Comicrosized Palmidrol INN) in Cats with Eosinophilic Granuloma and Eosinophilic Plaque: A Pilot Study. *Vet. Dermatol.* **2001**, *12*, 29–39. [[CrossRef](#)]
82. Aloe, L.; Leon, A.; Levi-Montalcini, R. A Proposed Autacoid Mechanism Controlling Mastocyte Behaviour. *Agents Actions* **1993**, *39*, C145–C147. [[CrossRef](#)] [[PubMed](#)]
83. Watkins, L.R.; Hutchinson, M.R.; Johnston, I.N.; Maier, S.F. Glia: Novel Counter-Regulators of Opioid Analgesia. *Trends Neurosci.* **2005**, *28*, 661–669. [[CrossRef](#)]
84. Liu, D.-Q.; Zhou, Y.-Q.; Gao, F. Targeting Cytokines for Morphine Tolerance: A Narrative Review. *Curr. Neuropharmacol.* **2019**, *17*, 366–376. [[CrossRef](#)]
85. Dozio, V.; Daali, Y.; Desmeules, J.; Sanchez, J.C. Deep Proteomics and Phosphoproteomics Reveal Novel Biological Pathways Perturbed by Morphine, Morphine-3-Glucuronide and Morphine-6-Glucuronide in Human Astrocytes. *J. Neurosci. Res.* **2022**, *100*, 220–236. [[CrossRef](#)]
86. Ma, R.; Kutchy, N.A.; Hu, G. Astrocyte-Derived Extracellular Vesicle-Mediated Activation of Primary Ciliary Signaling Contributes to the Development of Morphine Tolerance. *Biol. Psychiatry* **2021**, *90*, 575–585. [[CrossRef](#)]
87. Congiu, M.; Micheli, L.; Santoni, M.; Sagheddu, C.; Muntoni, A.L.; Makriyannis, A.; Malamas, M.S.; Ghelardini, C.; Di Cesare Mannelli, L.; Pistis, M. N-Acylethanolamine Acid Amidase Inhibition Potentiates Morphine Analgesia and Delays the Development of Tolerance. *Neurotherapeutics* **2021**, *18*, 2722–2736. [[CrossRef](#)] [[PubMed](#)]
88. Ruzicka, B.B.; Fox, C.A.; Thompson, R.C.; Meng, F.; Watson, S.J.; Akil, H. Primary Astroglial Cultures Derived from Several Rat Brain Regions Differentially Express μ , δ and κ Opioid Receptor mRNA. *Mol. Brain Res.* **1995**, *34*, 209–220. [[CrossRef](#)] [[PubMed](#)]

89. Nam, M.H.; Han, K.S.; Lee, J.; Bae, J.Y.; An, H.; Park, S.; Oh, S.J.; Kim, E.; Hwang, E.; Bae, Y.C.; et al. Expression of M-Opioid Receptor in CA1 Hippocampal Astrocytes. *Exp. Neurobiol.* **2018**, *27*, 120. [[CrossRef](#)]
90. Sil, S.; Periyasamy, P.; Guo, M.L.; Callen, S.; Buch, S. Morphine-Mediated Brain Region-Specific Astrocytosis Involves the ER Stress-Autophagy Axis. *Mol. Neurobiol.* **2018**, *55*, 6713. [[CrossRef](#)]
91. Esposito, E.; Paterniti, I.; Mazzon, E.; Genovese, T.; di Paola, R.; Galuppo, M.; Cuzzocrea, S. Effects of Palmitoylethanolamide on Release of Mast Cell Peptidases and Neurotrophic Factors after Spinal Cord Injury. *Brain Behav. Immun.* **2011**, *25*, 1099–1112. [[CrossRef](#)]
92. Kempuraj, D.; Thangavel, R.; Selvakumar, G.P.; Zaheer, S.; Ahmed, M.E.; Raikwar, S.P.; Zahoor, H.; Saeed, D.; Natteru, P.A.; Iyer, S.; et al. Brain and Peripheral Atypical Inflammatory Mediators Potentiate Neuroinflammation and Neurodegeneration. *Front. Cell. Neurosci.* **2017**, *11*, 216. [[CrossRef](#)] [[PubMed](#)]
93. Shavit, Y.; Wolf, G.; Goshen, I.; Livshits, D.; Yirmiya, R. Interleukin-1 Antagonizes Morphine Analgesia and Underlies Morphine Tolerance. *Pain* **2005**, *115*, 50–59. [[CrossRef](#)] [[PubMed](#)]
94. Shen, C.H.; Tsai, R.Y.; Shih, M.S.; Lin, S.L.; Tai, Y.H.; Chien, C.C.; Wong, C.S. Etanercept Restores the Antinociceptive Effect of Morphine and Suppresses Spinal Neuroinflammation in Morphine-Tolerant Rats. *Anesth. Analg.* **2011**, *112*, 454–459. [[CrossRef](#)]
95. Raghavendra, V.; Rutkowski, M.D.; Deleo, J.A. The Role of Spinal Neuroimmune Activation in Morphine Tolerance/Hyperalgesia in Neuropathic and Sham-Operated Rats. *J. Neurosci.* **2002**, *22*, 9980–9989. [[CrossRef](#)]
96. Niu, Z.J.; Ma, J.G.; Chu, H.C.; Zhao, Y.; Feng, W.; Cheng, Y.W. Melanocortin 4 Receptor Antagonists Attenuates Morphine Antinociceptive Tolerance, Astroglial Activation and Cytokines Expression in the Spinal Cord of Rat. *Neurosci. Lett.* **2012**, *529*, 112–117. [[CrossRef](#)] [[PubMed](#)]
97. Kwiatkowski, K.; Popiolek-Barczyk, K.; Piotrowska, A.; Rojewska, E.; Ciapała, K.; Makuch, W.; Mika, J. Chemokines CCL2 and CCL7, but Not CCL12, Play a Significant Role in the Development of Pain-Related Behavior and Opioid-Induced Analgesia. *Cytokine* **2019**, *119*, 202–213. [[CrossRef](#)]
98. Zhang, Y.; He, J.; Zhao, J.; Xu, M.; Lou, D.; Tso, P.; Li, Z.; Li, X. Effect of ApoA4 on SERPINA3 Mediated by Nuclear Receptors NR4A1 and NR1D1 in Hepatocytes. *Biochem. Biophys. Res. Commun.* **2017**, *487*, 327–332. [[CrossRef](#)]
99. Grek, C.L.; Townsend, D.M.; Uys, J.D.; Manevich, Y.; Coker, W.J.; Pazoles, C.J.; Tew, K.D. S-Glutathionylated Serine Proteinase Inhibitors as Plasma Biomarkers in Assessing Response to Redox-Modulating Drugs. *Cancer Res.* **2012**, *72*, 2383–2393. [[CrossRef](#)]
100. Park, J.; Masaki, T.; Mezaki, Y.; Yokoyama, H.; Nakamura, M.; Maehashi, H.; Fujimi, T.J.; Gouraud, S.S.; Nagatsuma, K.; Nakagomi, M.; et al. Alpha-1 Antichymotrypsin Is Involved in Astrocyte Injury in Concert with Arginine-Vasopressin during the Development of Acute Hepatic Encephalopathy. *PLoS ONE* **2017**, *12*, e0189346. [[CrossRef](#)] [[PubMed](#)]
101. Kanemaru, K.; Meckelein, B.; Marshall, D.C.L.; Sipe, J.D.; Abraham, C.R. Synthesis and Secretion of Active Alpha 1-Antichymotrypsin by Murine Primary Astrocytes. *Neurobiol. Aging* **1996**, *17*, 767–771. [[CrossRef](#)] [[PubMed](#)]
102. Kiss, D.L.; Xu, W.; Gopalan, S.; Buzanowska, K.; Wilczynska, K.M.; Rydel, R.E.; Kordula, T. Duration of A1-Antichymotrypsin Gene Activation by IL-1 Is Determined by Efficiency of IκBα Resynthesis in Primary Human Astrocytes. *J. Neurochem.* **2005**, *92*, 730. [[CrossRef](#)]
103. Vicuña, L.; Strohlic, D.E.; Latremoliere, A.; Bali, K.K.; Simonetti, M.; Husainie, D.; Prokosch, S.; Riva, P.; Griffin, R.S.; Njoo, C.; et al. The Serine Protease Inhibitor SerpinA3N Attenuates Neuropathic Pain by Inhibiting T Cell-Derived Leukocyte Elastase. *Nat. Med.* **2015**, *21*, 518–523. [[CrossRef](#)] [[PubMed](#)]
104. Bannon, M.J.; Johnson, M.M.; Michelhaugh, S.K.; Hartley, Z.J.; Halter, S.D.; David, J.A.; Kapatos, G.; Schmidt, C.J. A Molecular Profile of Cocaine Abuse Includes the Differential Expression of Genes That Regulate Transcription, Chromatin, and Dopamine Cell Phenotype. *Neuropsychopharmacology* **2014**, *39*, 2191–2199. [[CrossRef](#)] [[PubMed](#)]
105. Zamanian, J.L.; Xu, L.; Foo, L.C.; Nouri, N.; Zhou, L.; Giffard, R.G.; Barres, B.A. Genomic Analysis of Reactive Astrogliosis. *J. Neurosci.* **2012**, *32*, 6391–6410. [[CrossRef](#)] [[PubMed](#)]
106. Sun, W.; Kou, D.; Yu, Z.; Yang, S.; Jiang, C.; Xiong, D.; Xiao, L.; Deng, Q.; Xie, H.; Hao, Y. A Transcriptomic Analysis of Neuropathic Pain in Rat Dorsal Root Ganglia Following Peripheral Nerve Injury. *Neuromol. Med.* **2020**, *22*, 250–263. [[CrossRef](#)]
107. Maragakis, N.J.; Dykes-Hoberg, M.; Rothstein, J.D. Altered Expression of the Glutamate Transporter EAAT2b in Neurological Disease. *Ann. Neurol.* **2004**, *55*, 469–477. [[CrossRef](#)]
108. Middeldorp, J.; Hol, E.M. GFAP in Health and Disease. *Prog. Neurobiol.* **2011**, *93*, 421–443. [[CrossRef](#)]
109. Pekny, M.; Wilhelmsson, U.; Pekna, M. The Dual Role of Astrocyte Activation and Reactive Gliosis. *Neurosci. Lett.* **2014**, *565*, 30–38. [[CrossRef](#)]
110. Linnerbauer, M.; Rothhammer, V. Protective Functions of Reactive Astrocytes Following Central Nervous System Insult. *Front. Immunol.* **2020**, *11*, 573256. [[CrossRef](#)]
111. Beitner-Johnson, D.; Guitart, X.; Nestler, E.J. Glial Fibrillary Acidic Protein and the Mesolimbic Dopamine System: Regulation by Chronic Morphine and Lewis-Fischer Strain Differences in the Rat Ventral Tegmental Area. *J. Neurochem.* **1993**, *61*, 1766–1773. [[CrossRef](#)] [[PubMed](#)]
112. European Medicines Agency. Guideline Bioanalytical Method Validation. 2015. Available online: https://www.ema.europa.eu/en/documents/scientific-guideline/guideline-bioanalytical-method-validation_en.pdf (accessed on 12 January 2023).

113. ICH Q2(R2) Validation of Analytical Procedures. Available online: <https://www.ema.europa.eu/en/ich-q2r2-validation-analytical-procedures> (accessed on 12 January 2022).
114. Matuszewski, B.K.; Constanzer, M.L.; Chavez-Eng, C.M. Strategies for the Assessment of Matrix Effect in Quantitative Bioanalytical Methods Based on HPLC–MS/MS. *Anal. Chem.* **2003**, *75*, 3019–3030. [[CrossRef](#)] [[PubMed](#)]

Disclaimer/Publisher’s Note: The statements, opinions and data contained in all publications are solely those of the individual author(s) and contributor(s) and not of MDPI and/or the editor(s). MDPI and/or the editor(s) disclaim responsibility for any injury to people or property resulting from any ideas, methods, instructions or products referred to in the content.